1st International Conference on Engine Processes
6-7 June 2013

Ultra-Downsizing of Internal Combustion Engines

Victor Gheorghiu

Abstract

The downsizing of Internal Combustion Engines (ICE) is already recognized as a very suitable method for the concurrent enhancement of Indicated Fuel Conversion Efficiency (IFCE) and the lowering of CO_2 and NO_x emissions [1], [2]. In this report, ultra-downsizing is introduced as an even higher stage of development of ICE. Ultra-downsizing will be implemented here by means of real Atkinson cycles using asymmetrical crank mechanisms, combined with multi-stage high-pressure turbocharging and very intensive intercooling. This will allow an increase of ICE performance while keeping the thermal and mechanical strain strength of engine components within the current usual limits.

1. Introduction

The scarcity of oil and gas reserves and the global warming phenomenon both urge the automotive industry towards a decrease in fuel consumption and thus a reduction in CO_2 emissions. These factors will also determine the future R&D trends for ICE.
Downsizing of ICE means simultaneous decreasing the displaced volume (usually by reducing the number of cylinders) and increasing the Indicated Mean Pressure (IMEP) by means of turbocharging [1], [2]. This allows the preservation of power and torque performance while decreasing the engine size. As a result, a) the mechanical and thermal losses are reduced, b) the engine becomes lighter, leading to a drop in the overall weight of the vehicle, and c) the engine operates more within its optimum fuel consumption zone. The advantages offered by a) and b) hold true even for ICE used in hybrid propulsion systems, while the advantage c) is already a feature of full-hybrid vehicles.
The level of downsizing determines the strength of the thermal and mechanical strains of engine components. In order to avoid exceeding the usual limits, either the boost pressure or the Volumetric Compression Ratio (VCR) must be reduced accordingly. As a consequence, the whole potential of downsizing is not achieved and the IFCE and IMEP remain at a low level.
The current ICEs have classical (symmetrical) crank mechanisms (i.e. all strokes of equal length) and follow the Seiliger cycles. Atkinson cycles have been used so far mostly with these symmetrical crank mechanisms, where the intake valves are closed very late in the cycle [3] [4]. Thus, a part of the charge sucked into the cylinder is pushed back to the intake pipes, and the effective compression stroke is decreased. This implementation of *Quasi-Atkinson cycle* shows no noticeable improvements of the IFCE (see [3] to [6] for more details).

The Ultra-Downsizing (UD) is defined as a total concept consisting of several objectives and the measures required for its successful implementation. The main objectives of UD are increase the efficiency and the effective mean pressure, while reducing the emissions - particularly CO_2 and NO_x - in compliance with the usual thermal and mechanical strain limits of the engine components.
The required measures for implementing of UD are processual, structural (constructive) and operational.
The *processual measures* include:

- the implementation of the *real Atkinson cycle*,
- the attempt to reach the maximum recovery of the exhaust gas enthalpy by using an optimized partition between the internal (inside the cylinder) and external (inside the turbocharger) compression (of the fresh charge) and expansion (of the exhaust gas),
- the optimization of the heat release and of the gas exchange processes etc.

The *structural measures* include:

- the use of an *asymmetric crank mechanism* with a (much) shorter compression stroke compared to expansion stroke,
- the variability of the compression and expansion ratios,
- the use of very high-pressure turbocharging with very intensive cooling of the fresh charge before it is sucked into cylinder etc.

The *operational measures* include:

- maintaining the stoichiometric mixture in SI engines and the decrease of the AFR with respect of soot limits in CI engines at every engine operating points (EOP), which would enable the use of either a 3-way catalytic converter for NO_x reduction or a less frequent regeneration of the NO_x storage catalytic converter,
- the continuous adjustment of the compression ratio to the available boost pressure for performing the load control without throttling and/or leaning and stratifying of the mixture,
- shutting down the thermodynamic cylinder by shutting off the fuel supply and by significantly reducing the compression ratio etc.

2. Implementation of Quasi-Atkinson cycle on ICEs with classical (symmetrical) crank mechanism

2.1 Known implementations of the Quasi-Atkinson cycle

2.1.1 Aspirated engines

The market share of hybrid vehicles, most of them using Spark Ignition (SI) engines, has been steadily increasing over the past years. For example Toyota uses in its Prius II and III a SI engine which tries to achieve a higher IFCE by using a Quasi-Atkinson cycle. In this implementation of the Atkinson cycle the intake valve is kept open for a large part of the compression stroke and the volumetric compression ratio is enhanced. Consequently, in the initial stage of the compression stroke (when the piston begins to ascend), some of the air that had entered the cylinder is returned to the intake manifold, in effect delaying the start of compression. In this way, the expansion ratio is increased without increasing the effective compression ratio. Sophisticated variable valve timing is used to carefully adjust the intake valve timing to op-

erating conditions in order to reach maximum efficiency. Many variants of this implementation of the Atkinson cycle were evaluated in detail in [4]. In order to eliminate the influence of the heat exchange between the compared variants, which is difficult to control, the cylinder is henceforth basically treated as adiabatic.
Fig. 1 presents the IFCE above the Crank Angle (CA) for this Quasi-Atkinson cycle implementation (dashed curve) and for the Seiliger cycle. The Quasi-Atkinson cycle is derived from the Seiliger cycle by means of a 100°CA delaying of the intake valve closing ("ic") and by increasing the VCR by 90%.

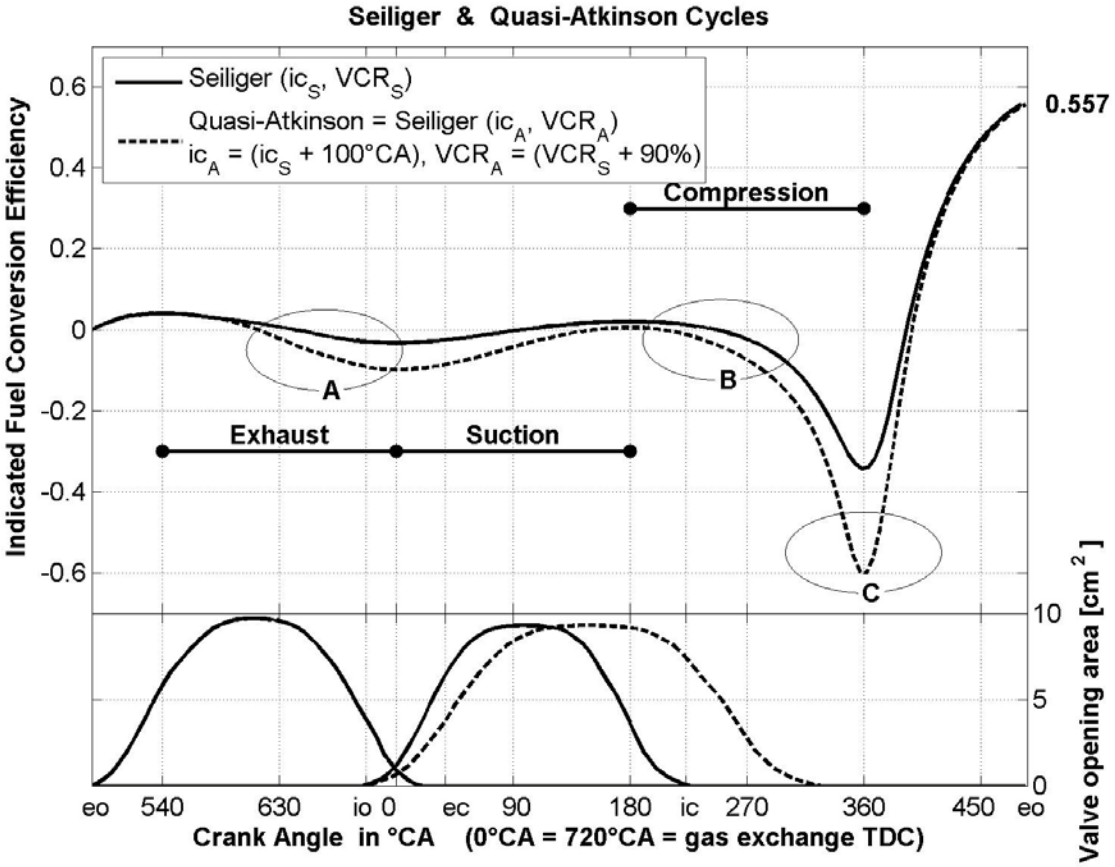

Fig. 1: Indicated Fuel Conversion Efficiency, Crank Angle (IFCE,CA) - Diagram

The pushing out of residual gases during the exhaust stroke consumes more piston work in the Quasi-Atkinson cycle (see A areas in Fig. 1) because of the lower pressure at the exhaust valve opening (see exhaust valve opening "eo" positions in Fig. 2) and consequently of the sluggish cylinder emptying process. The oscillating air stream from and to the intake manifold through the intake valve port (see B area in Fig. 3), reduces considerably the IFCE (see B areas in Fig. 1) of the cycle. Although the compression work in this Quasi-Atkinson cycle implementation is greater (because of the 90% increase of the VCR; see C area of Fig. 1), the increased VCR shows a very positive effect during the expansion stroke so that, finally, the IFCE level of the Seiliger cycle is reached.
One can conclude that the IFCE gain of this kind of Atkinson cycle implementation is modest and largely dependent on the fine tuning of all parameters (valve timing etc.). In addition the specific power of the engine is low because of the lower retained mass of fresh change in cylinder before compression (see Fig. 3).

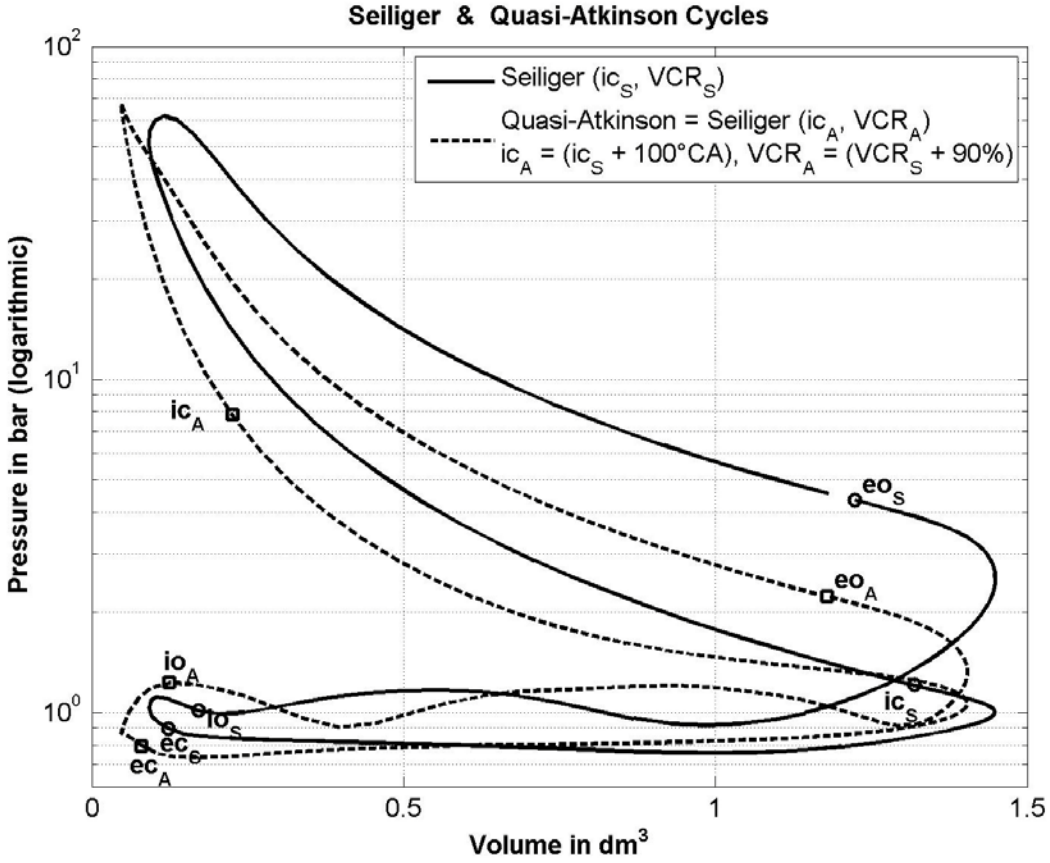

Fig. 2: Pressure (logarithmic), Volume (log(p),V) - Diagram

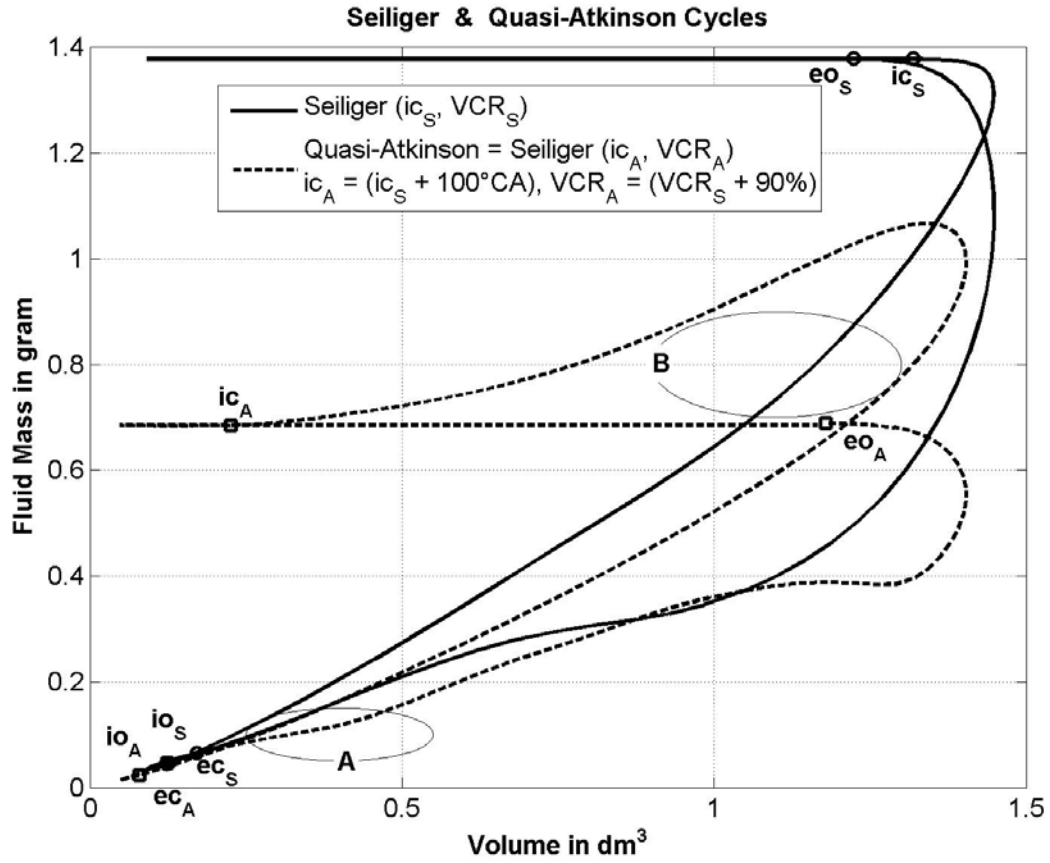

Fig. 3: Fluid Mass, Volume (m,V) - Diagram

This means that a relatively large (due to the large displacement) and therefore heavy engine is needed to power the vehicle. The most IFCE improvement in the case of Prius II and III is obtained by means of sifting the EOP in areas with maximal IFCE. For these reasons, this implementation of the Atkinson cycle is suitable only for hybrid vehicles, where the engine - because it is not directly linked mechanically to the wheels - works only in its best operating range.

2.1.2 Turbocharged engines

First, we analyze the commonly used practice of concomitant suction delaying and the increase in boost pressure. The number of parameters influencing the turbocharged engines becomes much higher compared to the aspirated engines. As a consequence, the effort to achieve the combinations of parameters which maximize the IFCE (η_i in the table from Fig. 5) of such engine cycles becomes much bigger. The simulation tool used here is the BOOST®, from AVL Co.

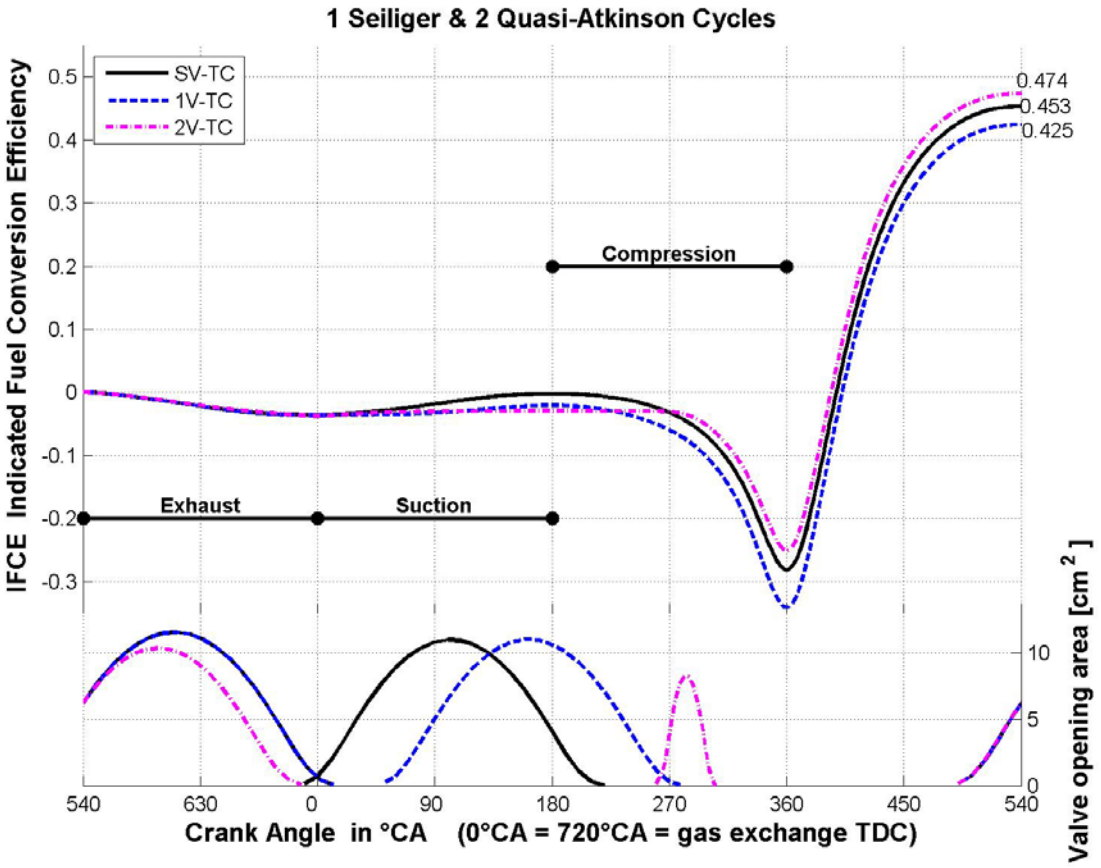

Fig. 4: Indicated Fuel Conversion Efficiency, Crank Angle (IFCE,CA) - Diagram

The simulation results for the Quasi-Atkinson cycle implementation (labeled here as 1V-TC), where the intake valve closing is 60°CA delayed, are presented in Figures 4 to 7. Due to the delay in suction, the gas exchange processes are very different from the standard version of the Seiliger cycle (labeled here as SV-TC). The boost pressure (p_C) is increased to achieve nearly the same filling rate of the cylinder (m_a) (see Fig. 7) and thus the same IMEP (p_i in the table from Fig. 5).
In the Quasi-Atkinson cycle implementation labeled 2V-TC, the suction is much more delayed and a very high charge pressure (of more than 16 bars) is taken into consid-

eration. Due to the delayed suction less mass is aspirated into cylinder (see Fig. 7). For improving the indicated IFCE of this cycle, the VCR is increased by 22% compared to the Seiliger cycle (SV-TC). Special characteristics of the 2V-TC Quasi-Atkinson cycle implementation are: a) the rest gases are expanded during the suction stroke and then compressed, as in the Miller cycle [3], [7] and b) the suction of fresh charge starts first, after the full completion of the suction in Seiliger cycle, and takes a very short time. Unfortunately, in order to achieve the same maximum values of pressure and temperature on both cycles at virtually the same IMEP, the AFR (λ in the table from Fig. 5) must be adapted in this case. The placement of the combustion phase in the cycle is identical to the Seiliger cycle. The simultaneous matching of all the parameters (i.e. maximum values of pressure and temperature, IMEP and AFR) is very difficult and time-consuming to achieve. The difference between the AFR values of both cycles is quite low and for this reason the EOP can be deemed to correspond to full load in both cycles. The fresh charge mass retained in cylinder is much lower in the 2V-TC Quasi-Atkinson cycle (see Fig. 7). During exhaust stroke, there are no major differences in IFCE between the cycles (see Fig. 4).

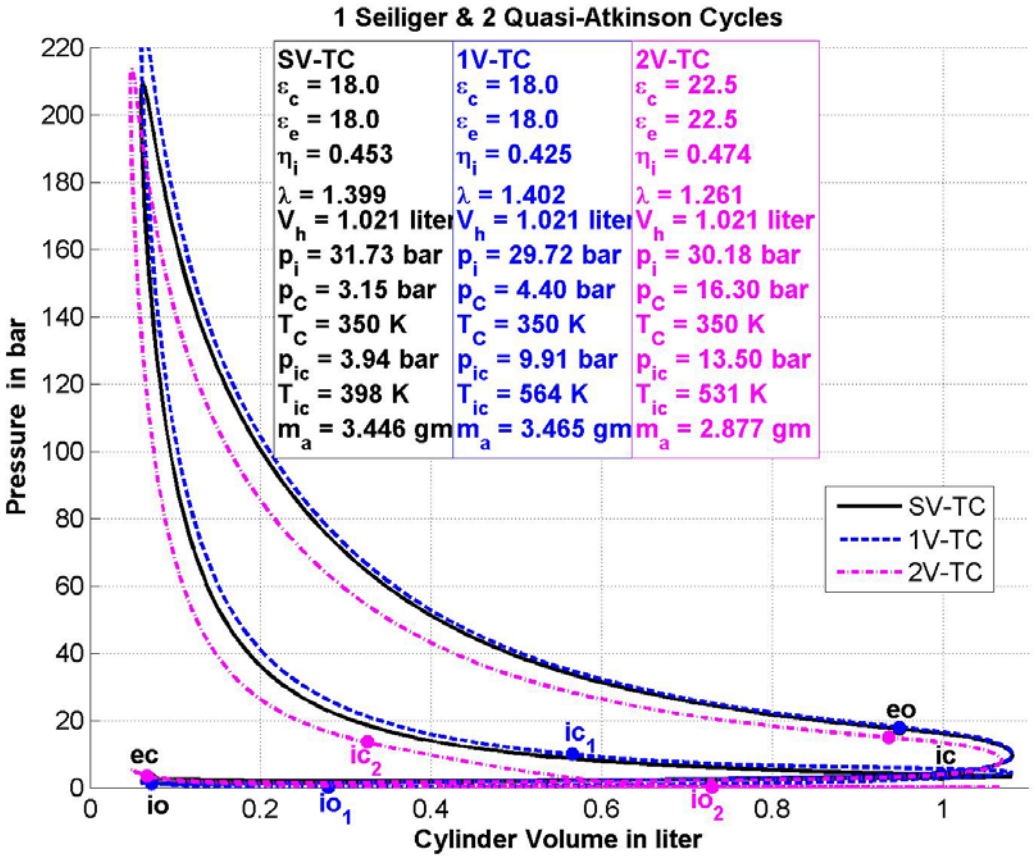

Fig. 5: Pressure, Volume (p,V) - Diagram

The major impact of the decrease in compression work in the Quasi-Atkinson cycle can be seen clearly after the closing of the intake valve (see Fig. 4). In short, although the boost pressure in the 2V-TC Quasi-Atkinson cycle implementation is more than five times higher at virtually the same IMEP, only a minor improvement of the IFCE can be detected. For this reason, the implementation of such Quasi-Atkinson cycles does not represent a suitable solution. Therefore, a new approach is needed to implement a real Atkinson cycle.

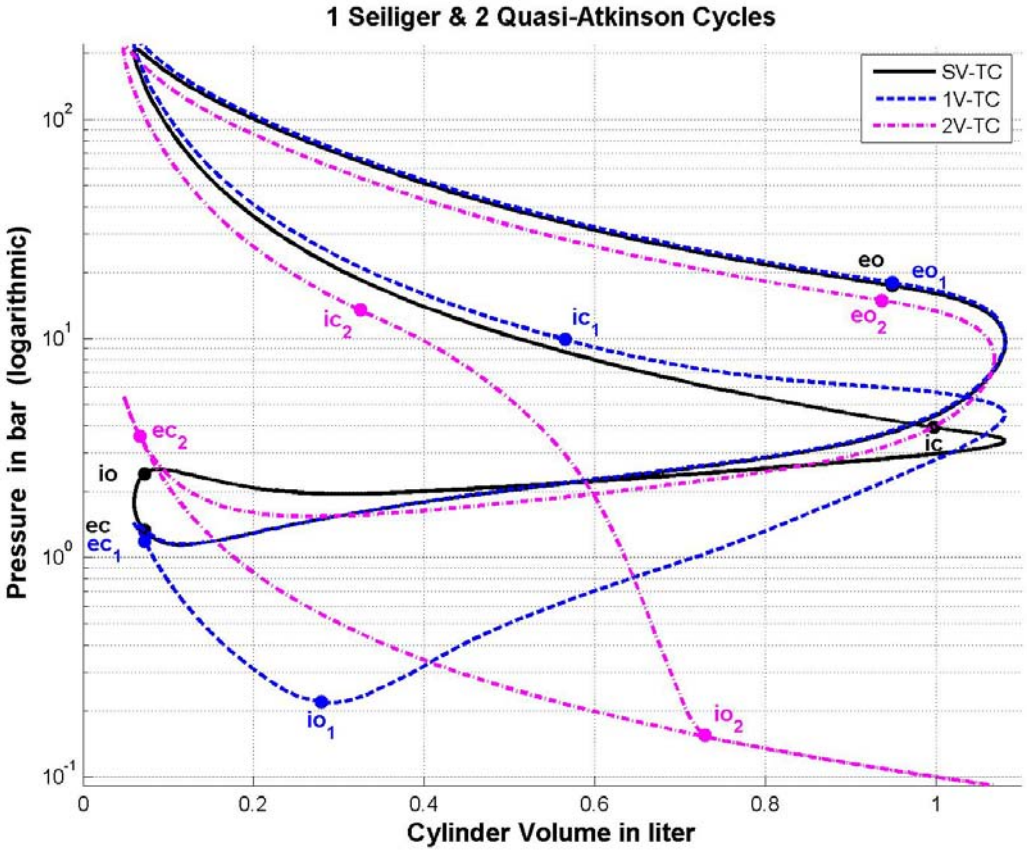

Fig. 6: Pressure (logarithmic), Volume (log(p),V) - Diagram

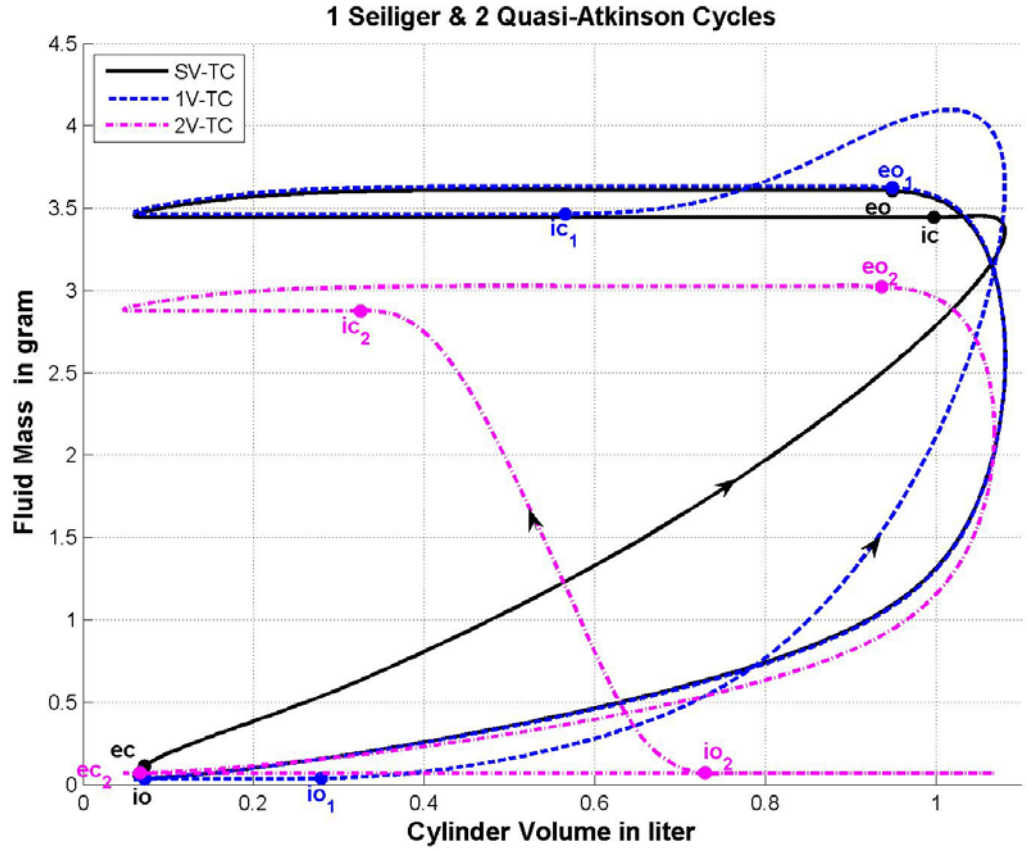

Fig. 7: Fluid Mass, Volume (m,V) - Diagram

3. Implementation of the Real-Atkinson cycle on ICEs with asymmetrical crank mechanisms

In order to realize a strict Atkinson cycle - i.e. shortened compression and extended expansion - a special crankshaft drive is proposed, which permits geometrically different strokes for compression and expansion (see Fig. 8 for aspirated engines [4], respectively 12A and 12B for supercharged engines [5], [6]). The design of this crankshaft drive is not the subject of this investigation (because it is still in the application stage of the patenting process) and it is therefore not described here. Its mechanical efficiency is estimated to be more than 96%. Many other crank mechanisms with asymmetrical strokes are in the application stage or have already been patented.

3.1. Aspirated ICEs

The aim here is merely to estimate the potential for increasing the IFCE if the crankshaft drive from Fig. 8 is used. In other words, this strict implementation of the Atkinson cycle, labeled further on as Real-Atkinson, investigates the extent to which losses caused by the suction and partial expulsion of the fresh charge reduce the IFCE.

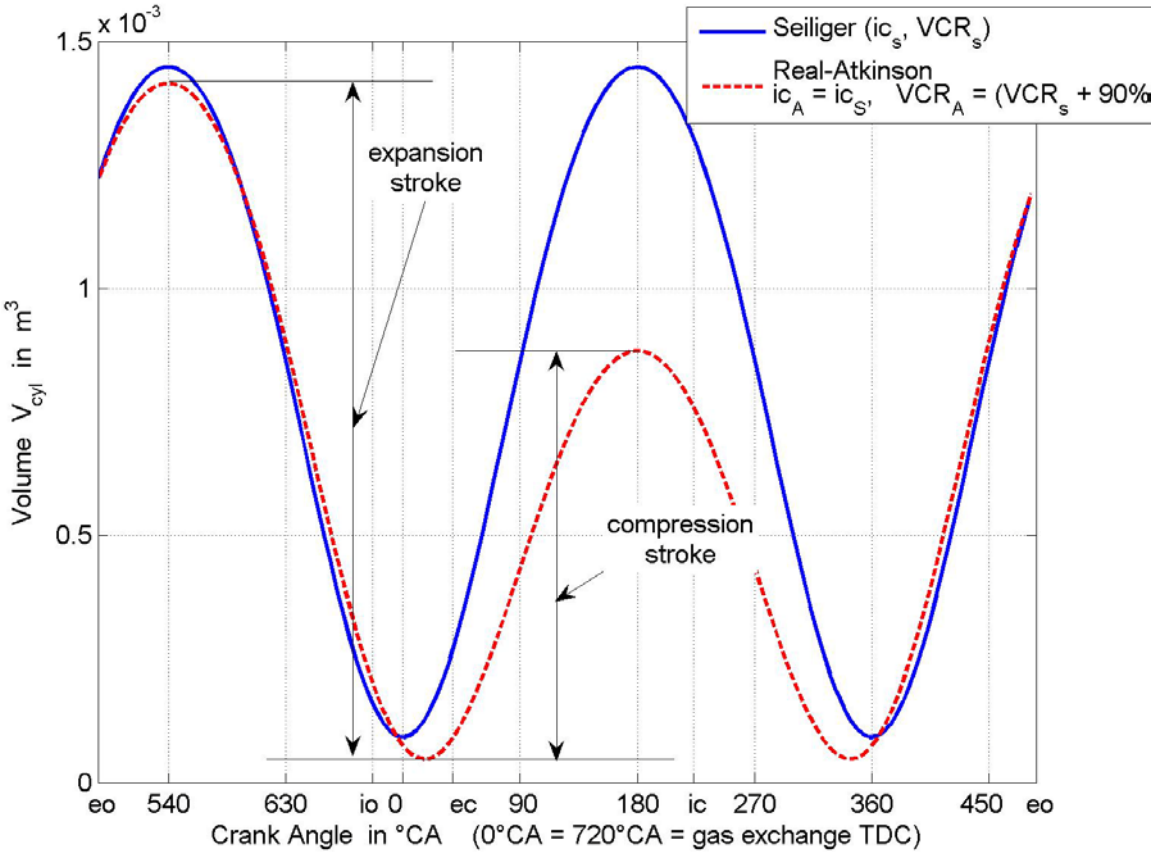

Fig. 8: Volume, Crank Angle (V,CA) - Diagram

As before, a comparison is made with the Seiliger cycle from Fig. 1 to 3. As the angle positions of the top dead centre are slightly shifted compared to the SV in this modified crankshaft drive, the closing angle of the exhaust valve in the 3V is also 20°CA delayed in order to avoid causing a large counter pressure during the valve

overlap time. The p,V-diagram is shown in Fig. 9, in which both the different compression and expansion strokes and also the increased compression ratio can clearly be recognized for the modified crankshaft drive.
An analysis of the IFCE-CA-diagram from Fig. 10 reveals that the IFCE is higher in the Real-Atkinson than in the Seiliger and Quasi-Atkinson cycles (see Fig. 1). The only factor which could have contributed to this is the elimination of the back and forth streaming through the intake valve (compare B areas in Fig. 1 and 9, since no other changes or parameter optimizations were made. The curve from Fig. 11 confirms that the entire aspirated gas mass of the Real-Atkinson cycle remains in the cylinder for combustion. Although the compression stroke is much shorter than in the Seiliger and Quasi-Atkinson cycles and the intake valve is open for a shorter time, the mass sucked in the Real-Atkinson cycle is roughly 6% greater than in the Quasi-Atkinson cycle (compare Fig. 3 and Fig. 11).
An analysis of the curves from Fig. 10 shows the same situation as in Fig. 1, where more piston work is needed in the Quasi-Atkinson and Real-Atkinson cycles for emptying the cylinder in comparison to the Seiliger cycle (see A areas in both figures). After the intake valve closes and the compression starts, the IFCE drops again sharply in the case of the Real-Atkinson cycle as a result of the increased VCR, but less sharply than in the case of the Quasi-Atkinson cycle (compare C areas in both figures) because of the elimination of back streaming through the intake valve (see B areas in both figures). A 15% increase of the IFCE is therefore achieved after compression and expansion in the Real-Atkinson cycle, compared to the Seiliger and Quasi-Atkinson cycles.

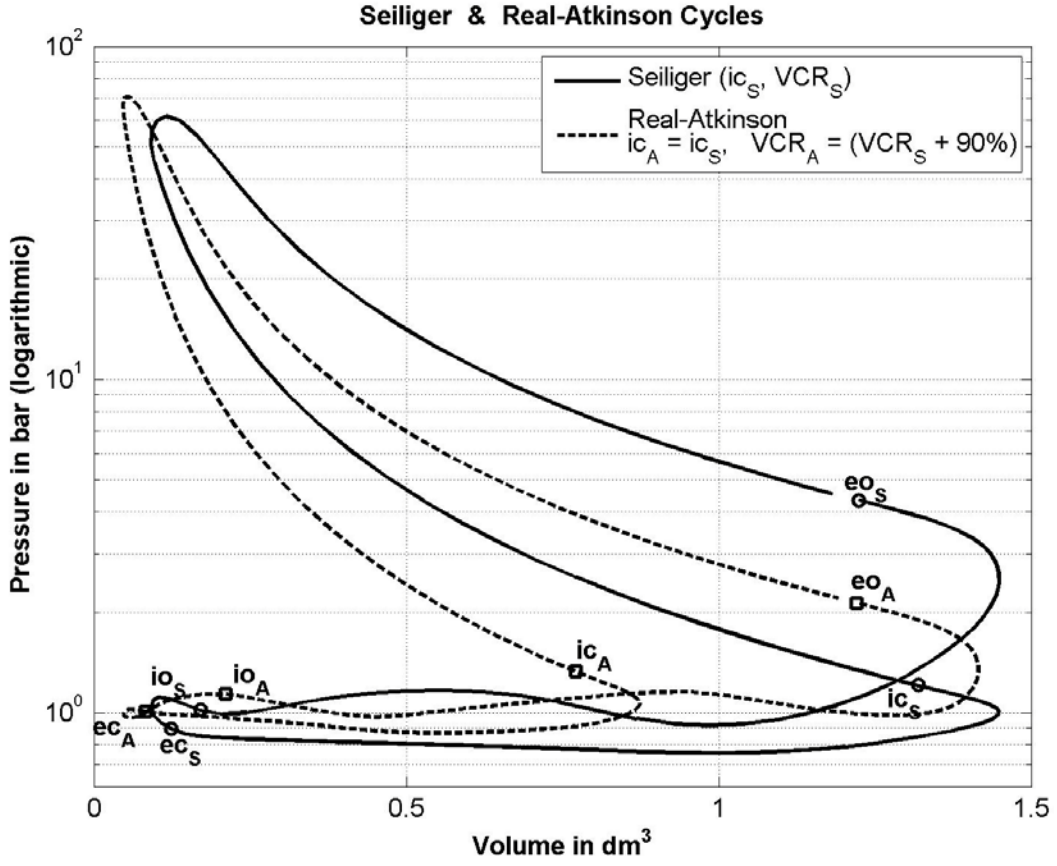

Fig. 9: Pressure (logarithmic), Volume (log(p),V) - Diagram

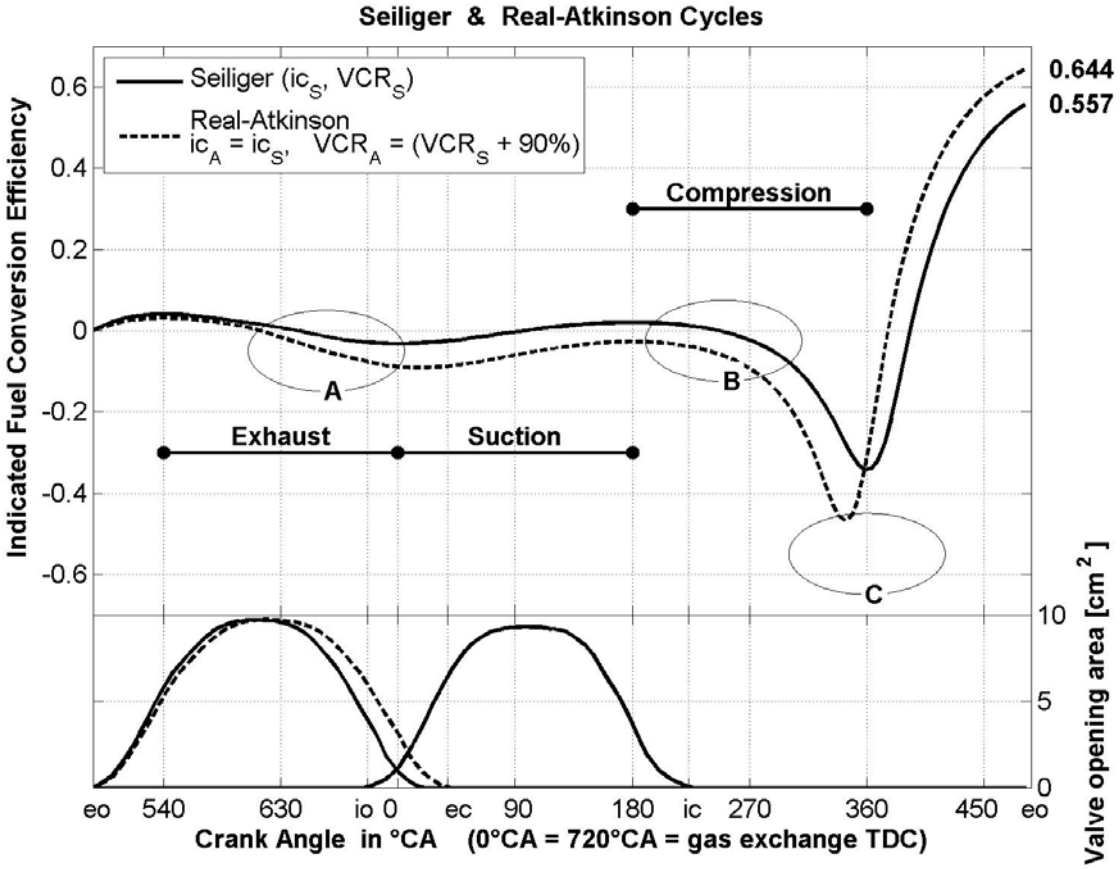

Fig. 10: Indicated Fuel Conversion Efficiency, Crank Angle (IFCE,CA) - Diagram

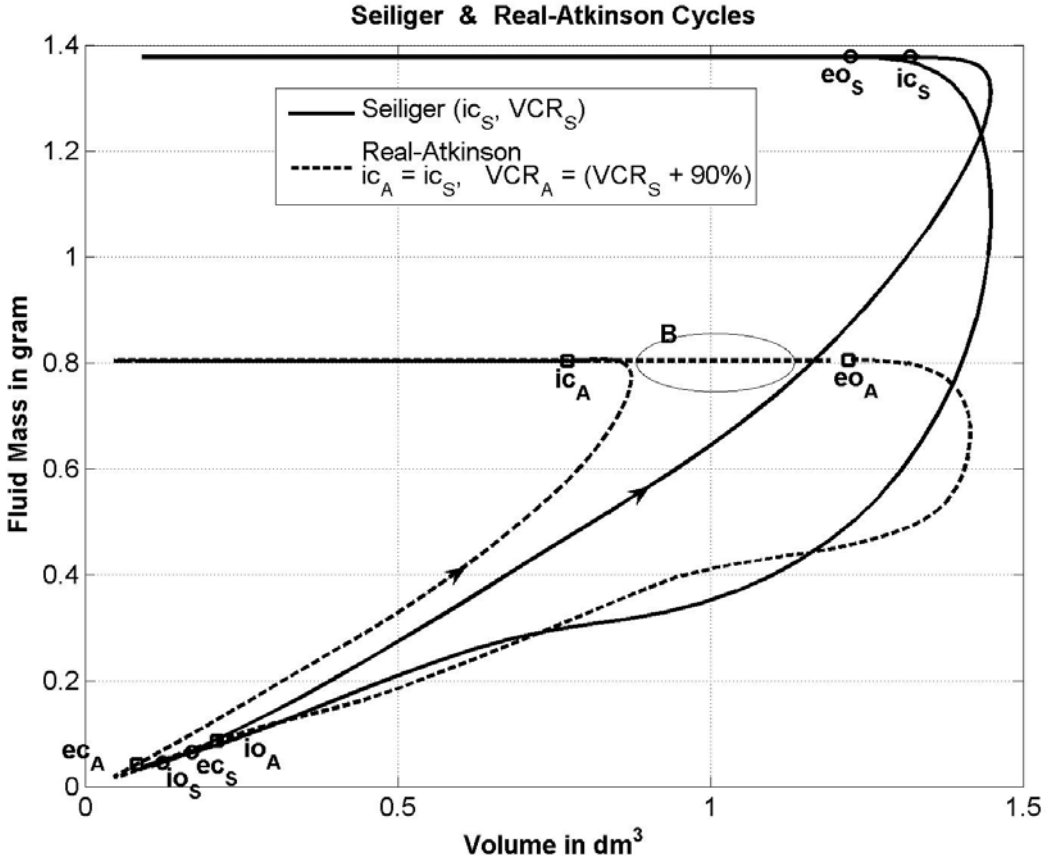

Fig. 11: Fluid Mass, Volume (m,V) - Diagram

3.2. Turbocharged engines

As before [4], [5], [6], the simulation tool used for turbocharged engines is the BOOST® tool, from AVL Co. The power balance of turbochargers determines the actual boost pressure level of the engine. The turbochargers (TC) are modeled for these investigations in a simple manner. It describes the expansion process in the turbines (Tx) by means of their discharge coefficients while the air compression within compressors occurs up to a maximum pressure ratio which depends on the available turbine output. To be able to simulate cycles with very high boost pressures as well, three intercooled TCs are placed in line (three-stage turbocharging, see Fig. 12). When the boost pressure required for preserving the pressure limit on the cycle is low, the superfluous TCs are kept for simplicity and comparability in use (i.e. are not bypassed). In this case the expansion and compression ratios of the turbines and compressors tend gradually toward 1, i.e. these TCs switch off themselves thermodynamically.

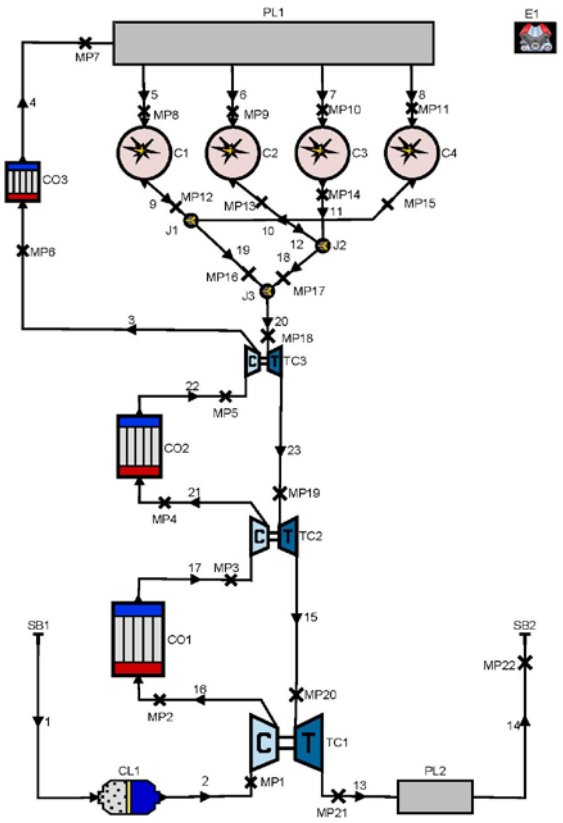

Fig. 12 BOOST model of a four cylinder turbocharged engine
Simple number denotes pipes, **Cx** = cylinder, **COx** = cooler, **TCx** = turbochargers, **PLx** = plenum, **Jx** = junctions, **CLx** = cleaner, **SBx** = system boundaries, **Ex** = engine and **MPx** = measuring points

The asymmetrical crank mechanism used here can realize the classical piston displacements for the Seiliger as well as for the Real-Atkinson cycles with various asymmetries between the compression and expansion strokes (see. Fig. 13A) and enable the variation of the VCR (see Fig. 13B).

The limitation of the maximum pressure during the cycle determines the VCR - boost pressure pair of parameters. If a relatively high boost pressure is desired, the VCR must be reduced accordingly in order to accomplish the maximum pressure limitation of the cycle. This will also decrease the IFCE since it is determined primarily by the VCR. Furthermore, the expansion in the cylinder occurs largely incompletely and the exhaust gases exit the cylinder with a still too high specific enthalpy, which decreases the IFCE even further. However, the expansion of exhaust gases in the turbines with its high specific enthalpy can be used only in part to drive the compressors and, therefore, to enhance the boost pressure because it exceeds the upper pressure limit of the cycle.

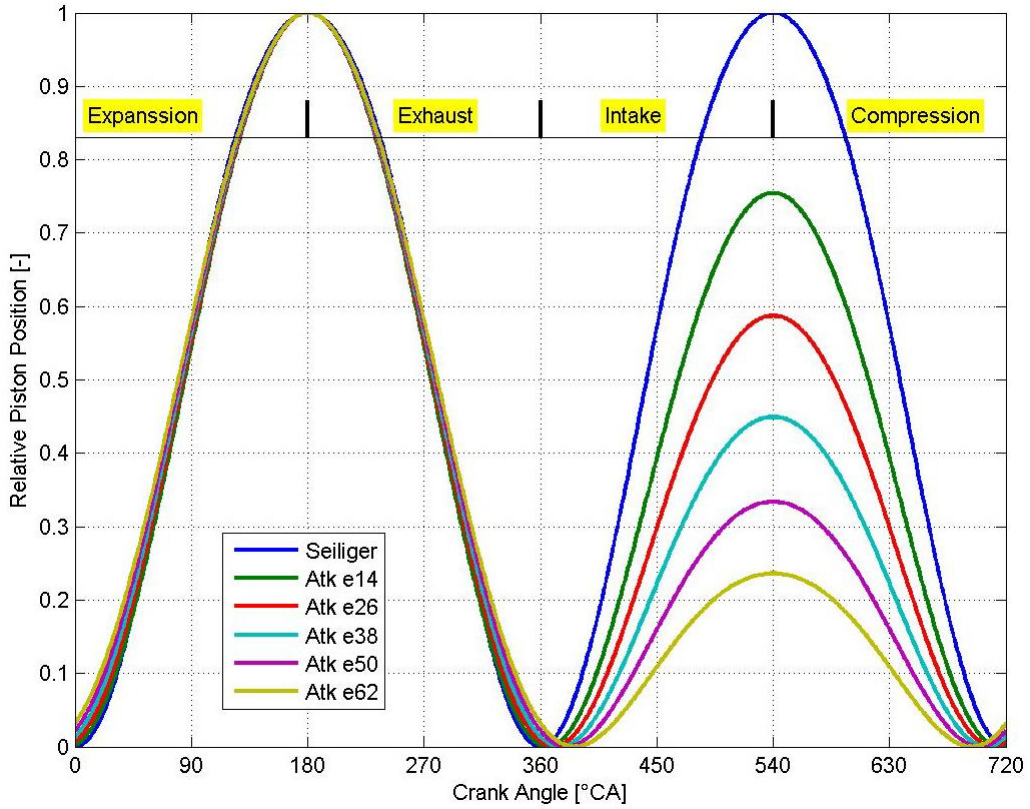

Fig. 13A Relative Piston Position, Crank Angle - Diagram used in the IC A

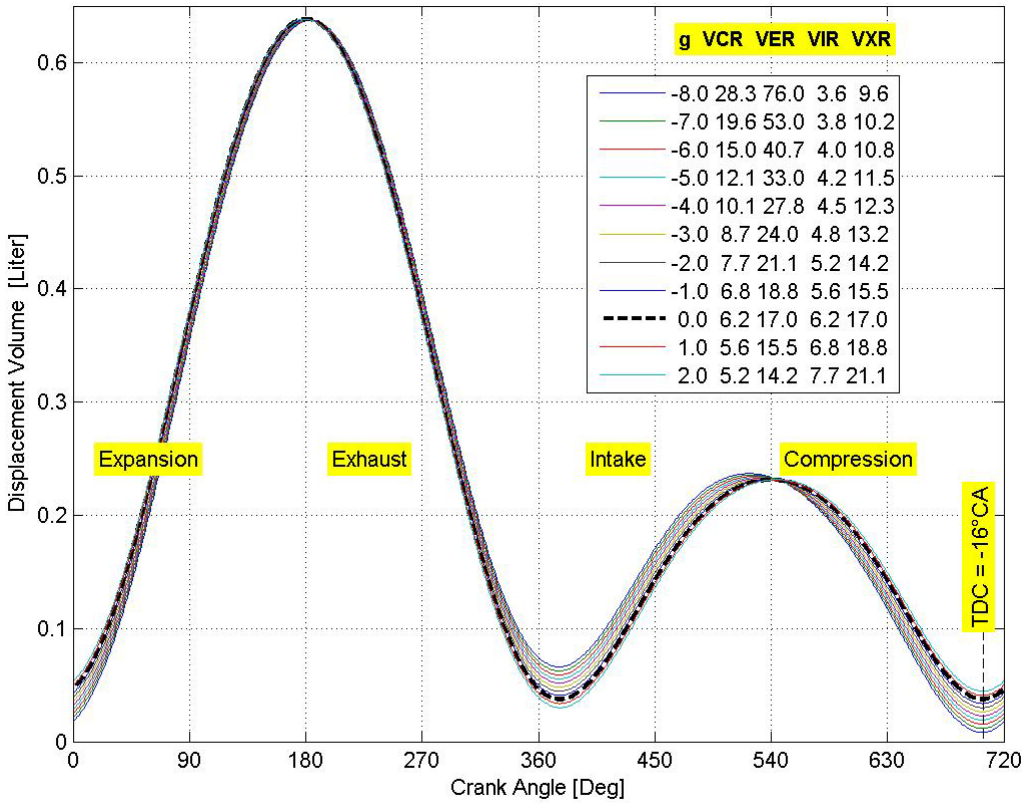

Fig. 13B Displacement Volume, Crank Angle - Diagram used in the IC B

The following facts can be used to summarize the current situation:
To raise the IFCE, most of the working gas expansion should occur within the cylinder. If, however, the expansion process occurs entirely within the cylinder (ideally, a full expansion occurs up to the ambient pressure), no additional boost pressure can be generated.
In order to increase the expansion part within the cylinder, the crank mechanism must provide a higher Volumetric Expansion Ratio (VER), which makes a long expansion stroke (and, therefore, an engine with a long piston displacement) necessary. However, that leads to a high IFCE but quite low indicated specific power (kW/L) and IMEP of the engine.
In order to simultaneously increase the IFCE and the IMEP, the engine must be turbocharged and the ratio between the expansions within the cylinder and within the turbines (i.e. between the internal and external expansions) must be optimized. To be able to optimize this ratio (i.e. between internal and external expansions) regardless of VCR, an asymmetrical crank mechanism is required in order to implement real Atkinson cycles.
The simulations are carried out in the following two investigation cases **(IC**) with the purpose of looking for the optimum ratio between the internal and external expansions, which leads simultaneously to maximizing the IFCE and enabling sufficiently high values of IMEP:
In the **IC A**, the simulated variants are based on a steady VER and a varied VCR. This means that the identical expansion and exhaust strokes are kept unchanged while the identical intake and compression strokes are varied significantly - by means of varying the eccentric radiuses "exx" (see legend of Fig. 13A) of the crank mechanism - in order to allow the modification of the ratio between internal and external expansion.
In the **IC B**, the simulated variants are based on a steady eccentric radius (e32) where VER, VCR, Volumetric Intake Ratio (VIR) and Volumetric Exhaust Ratio (VXR) are varied simultaneously by means of the parameter "g" (see the legend of Fig. 13B).
Most parameters of the BOOST model are selected for a hypothetical engine and are kept unchanged for all simulations. This includes parameters such as all geometrical dimensions (with the exception of the crank mechanism), valve timing, wall temperatures (300 K) and heat transfer coefficients (Re-analogy) of the pipes, as well as the efficiencies and pressure losses of the intercoolers (target efficiency = 0.75, target pressure drop = 5 kPa) and friction coefficients in the pipes (0.019). Likewise, the efficiency of the turbochargers (compressor efficiency = 0.75, turbocharger overall efficiency = 0.5), as well as the blow by gap size of the cylinder, frictional characteristic curve of the engine and AFR - the combustion parameter (see Table 1A) - are also included. A simple Vibe function is selected in order to model the combustion process. The different positions of the TDC in the Atkinson and Seiliger cycles (see Fig. 13A) are compensated by choosing a suitable start of combustion (SOC), so that combustion begins uniformly in all cycles at 15°CA before TDC.
The Table 1A shows the VER (volumetric expansion ratio), VCR (volumetric compression ratio), μ_{Tx} (turbine discharge coefficients), n (engine speed), AFR (air-fuel ratio), SOC (start of combustion), CD (combustion duration), m_{Vibe} (exponent of Vibe function for the cylinder heat release modeling), IFCE (indicated fuel conversion efficiency), IMEP (indicated mean pressure), max(p) and max(T) (maximum pressure

and temperature during the cycle), p_{MP8} and T_{MP8} (mean boost pressure and temperature; i.e. at the measuring point MP8, see Fig. 12) and p_{MP12} and T_{MP12} (mean exhaust back pressure and temperature; i.e. at MP12, see Fig. 12) for cylinder 1.

Cycle	VER	VCR	μ_{T1}	μ_{T2}	μ_{T3}	n	AFR	SOC	CD	m_{Vibe}
	-	-	-	-	-	rpm	kg/kg	°CA	°CA	-
Atk e14	27,0	20,6	0,480	0,258	0,161	3000	14,6	-21	86	1,5
Atk e26	27,0	16,2	0,430	0,231	0,144	3000	14,6	-24	86	1,5
Atk e38	27,0	12,7	0,335	0,180	0,112	3000	14,6	-30	86	1,5
Atk e50	27,0	9,7	0,256	0,138	0,086	3000	14,6	-36	86	1,5
Atk e62	27,0	7,1	0,199	0,106	0,067	3000	14,6	-42	86	1,5
Seiliger	7,0	7,0	0,330	0,177	0,111	3000	14,6	-15	86	1,5
Seiliger	15,0	15,0	0,620	0,333	0,208	3000	14,6	-15	86	1,5

Cycle	VER	VCR	IFCE	IMEP	max(p)	max(T)	p_{MP8}	T_{MP8}	p_{MP12}	T_{MP12}
	-	-	-	bar	bar	K	bar	K	bar	K
Atk e14	27,0	20,6	0,419	25,7	231	2209	3,02	336	2,79	867
Atk e26	27,0	16,2	0,423	28,2	234	2197	4,08	343	3,78	877
Atk e38	27,0	12,7	0,423	27,9	237	2182	5,13	346	4,79	877
Atk e50	27,0	9,7	0,413	26,7	235	2167	6,55	348	6,16	913
Atk e62	27,0	7,1	0,391	24,6	229	2152	8,78	356	8,07	915
Seiliger	7,0	7,0	0,301	57,9	232	2292	12,48	450	15,85	1396
Seiliger	15,0	15,0	0,383	42,1	232	2344	4,62	361	4,62	1127

Table 1A Parameter (top) and Performance (bottom) for IC A (comma means decimal point!)

The various parameters from Table 1A for the IC A and from Fig. 20B for the IC B are selected for the purpose of obtaining roughly the same maximum cylinder pressure max(p) ≈ 230 bar in all cycles (see Fig. 15A). In order to reach this state, the discharge coefficients of the three turbines (μ_{T1}, μ_{T2} and μ_{T3}) are varied according to a) the influence of the back pressure behind the cylinder (e.g. at the measuring point MP12 for cylinder 1; see Fig. 12) and of b) the boost pressure (e.g. at MP8 for cylinder 1). In order to reach approximately the same expansion rate in all three turbines, their discharge coefficients are set at the same level and compensated with the cross sections ratios of the turbine output pipes. Hence, only the discharge coefficient of the third turbine μ_{T3} is adapted for each cycle to meet the cylinder peak pressure limit, since this sets the level of the other two discharge coefficients μ_{T2} and μ_{T1} (see Table 1A and Fig. 20B).

3.2.1 Simulation results and trends for the IC A

All Atkinson cycles show better IFCE values than the Seiliger cycles (see Fig. 14A). However, the Seiliger cycles reach higher IMEP values because of the longer intake stroke and, therefore, the larger gas mass sucked in (see Fig. 19A). Furthermore, higher boost pressures p_{MP8} are required in both the Atkinson and Seiliger cycles in order to hold the parameter max(p) steady when the VCR is reduced (see Table 1A). The comparison of the Atk e62 (with VCR = 7.1) and Seiliger (with VCR = 7) cycles shows that a) the Atkinson cycle has a 30% higher IFCE and reaches 58% less IMEP and b) the Seiliger cycle needs a 30% higher boost pressure (p_{MP8} in Table

1A) and must overcome a 50% higher cylinder back pressure - i.e. before T3 (p_{MP12} in Table 1A). Moreover, the comparison of the Atk e38 & e26 (with VCR = 12.7 respective = 16.2) and Seiliger (with VCR = 15) cycles shows that the Atkinson cycles have a 10% higher IFCE (although the maximum cylinder temperature max(T) is ca. 160 K, i.e. 7% lower) and a 34% lower IMEP. The highest IFCE value for the Atkinson cycles is not reached in the variant with the highest VCR, but in the variant where the VCR is about 50% of the VER. Consequently, the optimum variant features an intake stroke equal to approx. 50% of the expansion stroke.

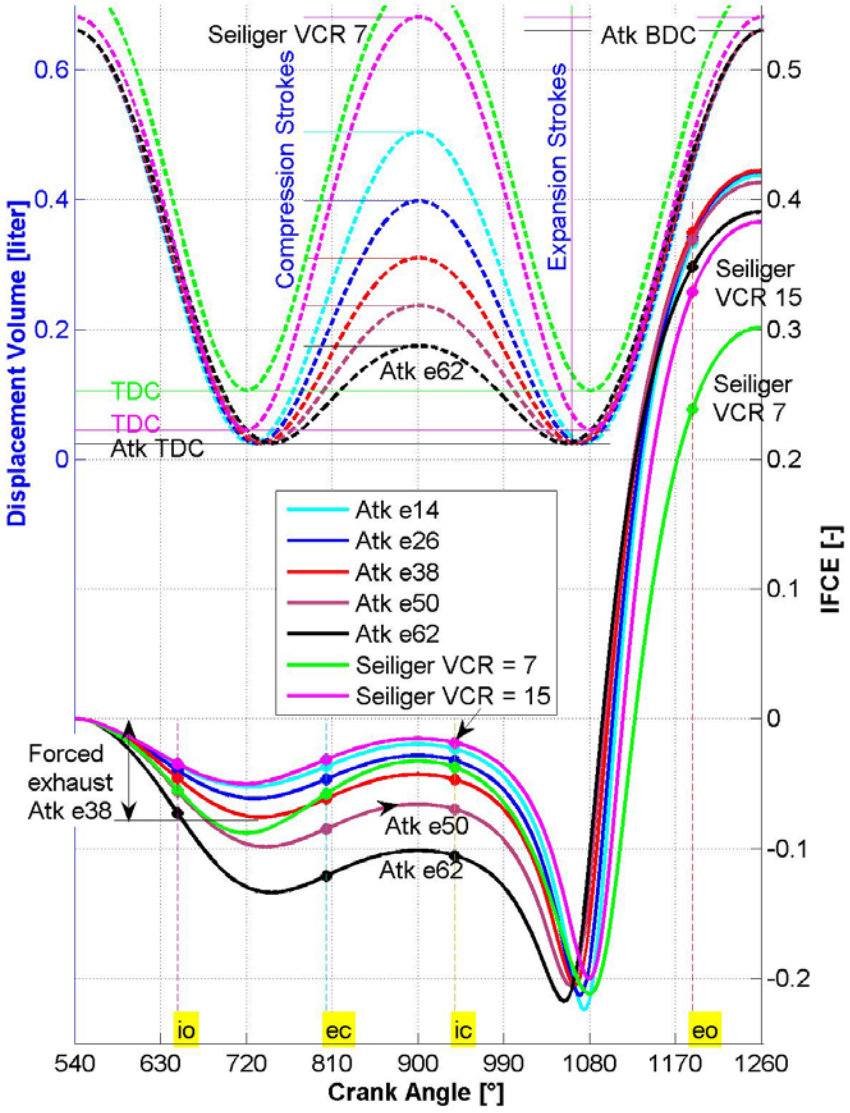

Fig. 14A: Indicated Fuel Conversion Efficiency, Crank Angle (IFCE,CA) - Diagram (top curves with right axis) and Displacement Volume, Crank Angle (V,CA)-Diagram (bottom curves with left axis)

Some diagrams are introduced and analyzed below in order to determine the cause of these trends. The pressure-volume (p,V) diagram of all cycles is presented in Fig. 15A and the pressure-specific volume (p,v) diagram of the intake and the exhaust gas paths of each Seiliger and Atkinson cycle are presented in Fig. 16A. It can be inferred from Table 1A, as well as recognized in Fig. 15A and 16A, that the Seiliger

cycle where the VCR = 7 needs the highest boost pressure to reach the desired max(p) ≈ 230 bar (because of its low VCR). The consequences are an extremely high back pressure p_{MP12} (see Fig. 16A) and falling ISFC because of the very intensive exhaust work required to push the exhaust gases out of the cylinder (see in Fig. 15A the curve up to exhaust valve closing "ec" point). Therefore, this cycle occurs exclusively in the pressure range above 10 bar. For the Atkinson cycle Atk e38, this situation is reversed (see Table 1A and Fig. 15A and 16A for comparison). This cycle occurs exclusively in the pressure range above 5 bar.

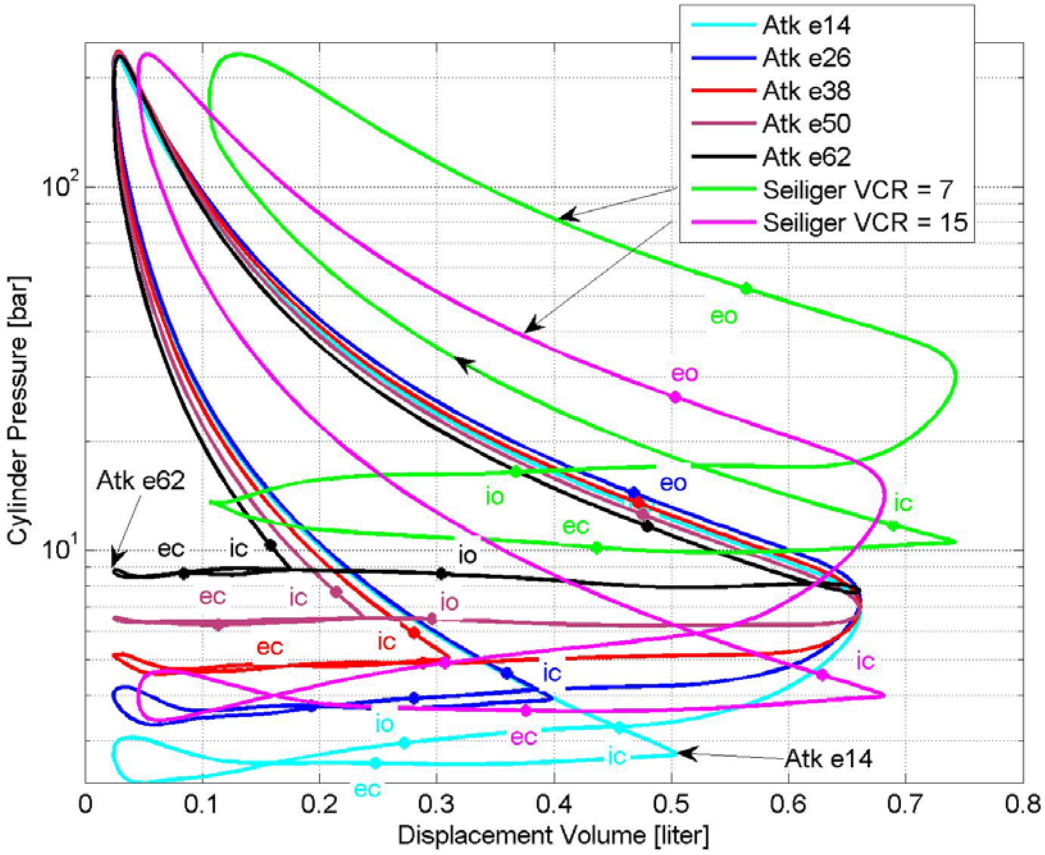

Fig. 15A: Pressure (logarithmic), Volume (log(p),V) - Diagram

The differences between both cycles can be clearly seen in the intake and exhaust gas paths. Fig. 16A and 17A show the three-stage compression of the air and all the states after passing through each compressor and intercooler (with the associated pressure losses). Fig. 16A and 18A show the three-stage expansion of the exhaust gases in the turbines. Fig. 18A shows, that the discharge coefficients are properly adapted between the turbines because the expansion occurs almost linearly in all three stages.

The air compression and the exhaust gas expansion for the cycle Atk e38 occur mostly in TC3 (see Fig. 16A and 17A) because the exhaust gas pressure at the MP18 point (i.e. before T3, see Fig. 16A and 18A) is too low (see also Table 1A) to be able to adequately drive T2 and T1. Consequently, the exhaust gases compress partly in T2 and T1 instead of expanding (see MP19 to MP21 in Fig. 16A). No modification of the IFCE sequence between variants is obtained by deleting TC1 from the BOOST model (i.e. there is no need to remove the unnecessary TC in these simulations).

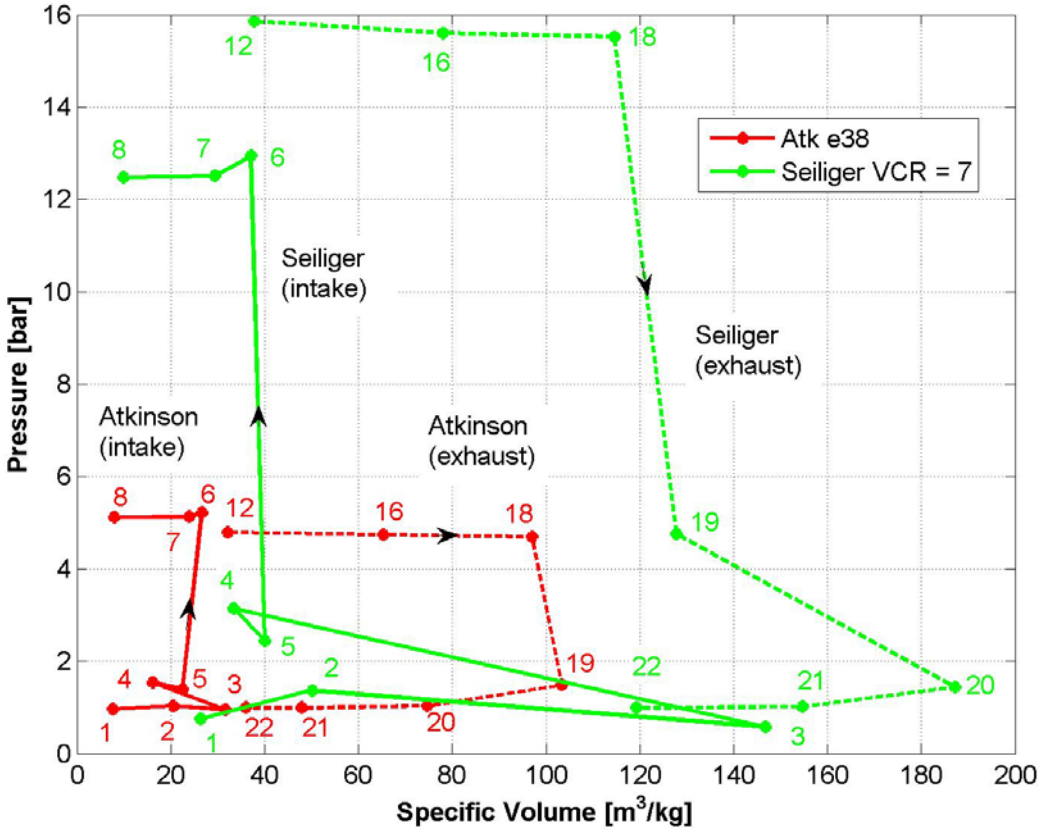

Fig. 16A: Pressure, Specific Volume (p,v) - Diagram

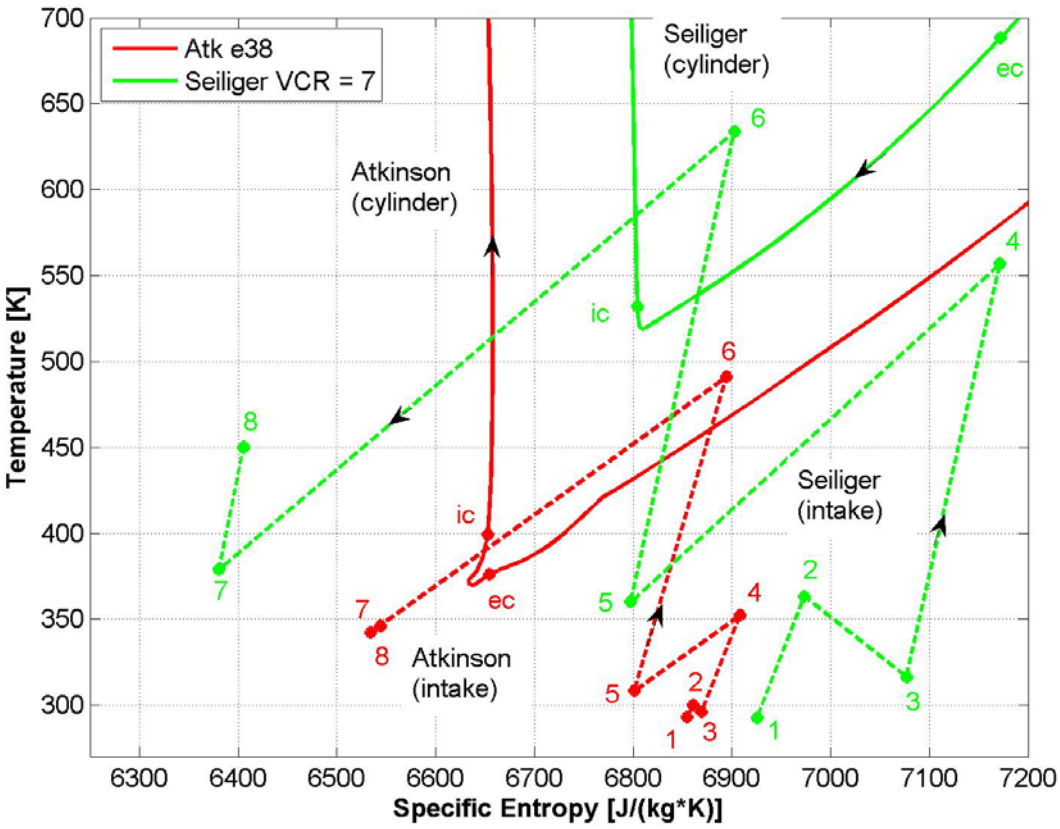

Fig. 17A: Temperature, Specific Entropy (T,s) - Diagram in Cylinder & Intake Path

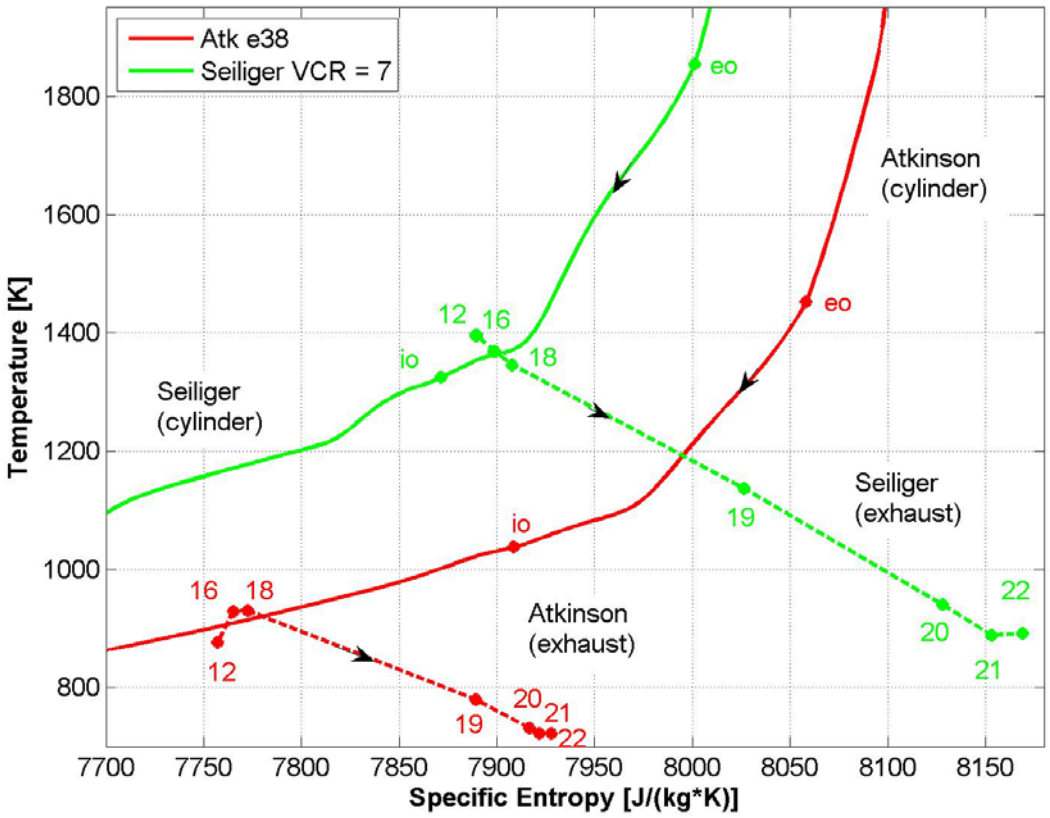

Fig. 18A: Temperature, Specific Entropy (T,s) - Diagram in Cylinder & Exhaust Path

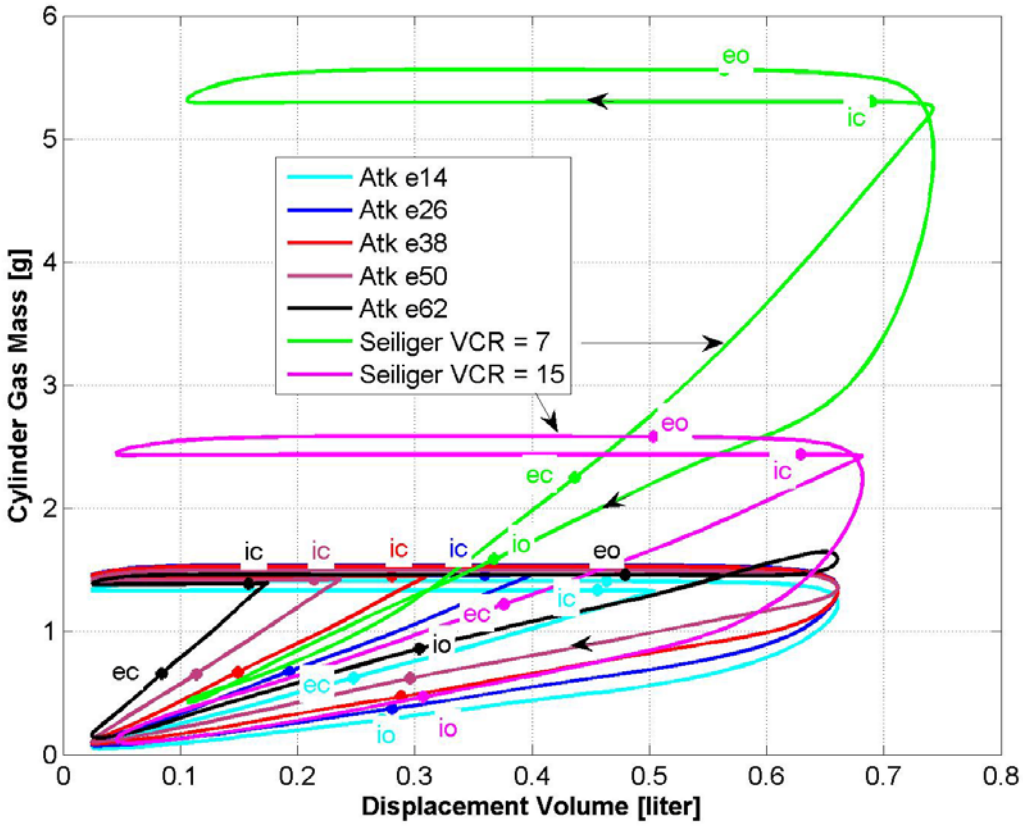

Fig. 19A: Fluid Mass, Volume (m,V) - Diagram

In all Atkinson cycles, the sucked intake gas mass changes minimally (see the red circle area on the left side of Fig. 19A), i.e. IMEP follows preponderantly IFCE variation and is, for the most part, independent of the boost pressure (p_{MP8}) variation.

3.2.2 Simulation results and trends for the IC B

A number of trends become clear after analyzing the parameter and performances presented in Fig. 20B.

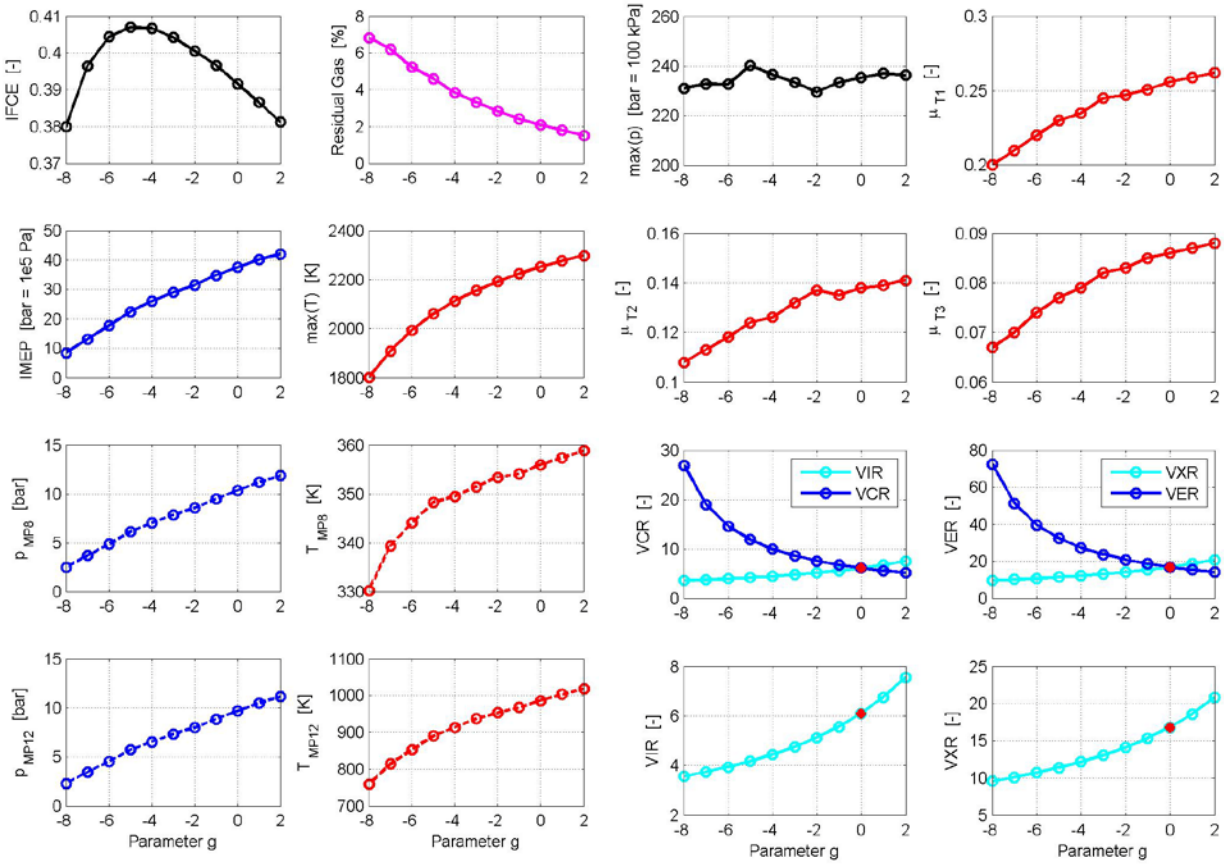

*Fig. 20B Parameters (left) and Performance (right) for the **IC B** over Parameter "g"*

This type of crank mechanism – which permits the VCR variation (in this case via parameter "g") – enables the implementation of Real-Atkinson cycles for part and full-load operating points (OPs), where the IMEP varies between 8.5 and 42 bar, even with the stoichiometric AFR and without throttling. Moreover, the IFCE in all these OPs only varies within a 6% band (related to its maximum value, see also Fig. 20B and 21B). In all these OPs, the maximum cylinder pressure remains at approx. 230 bar and the maximum cylinder temperature varies between 1800 and 2300 K (see Fig. 20B and 22B). The optimization of the heat release could significantly reduce the maximum cylinder temperature. In variant "g+2" (see legend), the maximum boost pressure (p_{PM8}) reaches nearly 12 bar, while the boost temperature (T_{PM8}) does not exceed 360 K (see Fig. 20B). In this case, the cylinder is filled to maximum (see Fig. 23B). As a result of the extended expansion within the cylinder (see Fig. 11B) the exhaust gas temperatures before turbine T3 (T_{MP12}) only reach a maximum of 1000 K. This means that the turbine wheel does not need to be protected (e.g. by making the mixture leaner) against a higher gas temperature, but, at the same time,

a higher exhaust gas pressure is required before T3 (p_{MP12}) in order to achieve the desired boost pressure (p_{MP8}).

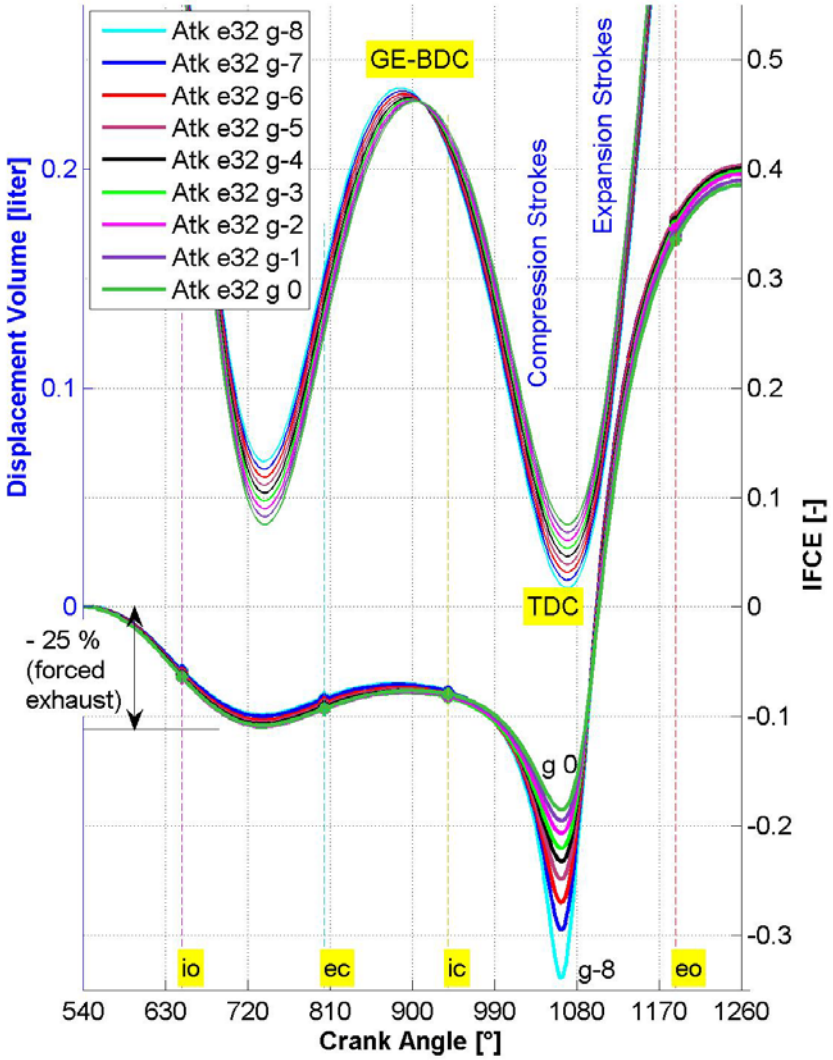

Fig. 21B: Indicated Fuel Conversion Efficiency, Crank Angle (IFCE,CA) - Diagram (top curves with right axis) and Displacement Volume, Crank Angle (V,CA)-Diagram (bottom curves with left axis)

The required higher exhaust gas pressure before T3 (p_{MP12}) (i.e. the cylinder back pressure) significantly diminishes the IFCE (i.e. by approx. 25%, see IFCE variation in Fig. 12B between 540°CA and the "ec" position). The load independence of these IFCE losses is quite unexpected, but if the difference between the cylinder pressure at "eo" and the back pressure (p_{MP12}) in Fig. 13B is noted, the positive effect of the exhaust gases released from the cylinder (i.e. of the free exhaust) becomes evident. An additional optimization of the valve timing can considerably reduce the back pressure and, therefore, these IFCE losses. The residual gas concentration decreases, while the VXR and boost pressure increase (see Fig. 20B). The increase in the VXR makes the cylinder exhaust more complete and the increase in boost pressure favors the scavenging of residual gases from the cylinder. The IMEP enhancement – from 8.5 to 42 bar, while AFR remains unchanged (here stoichiometric) and IFCE only varies within a 6% band – is the result of more gas mass aspirated into the cylinder (see Fig. 23B).

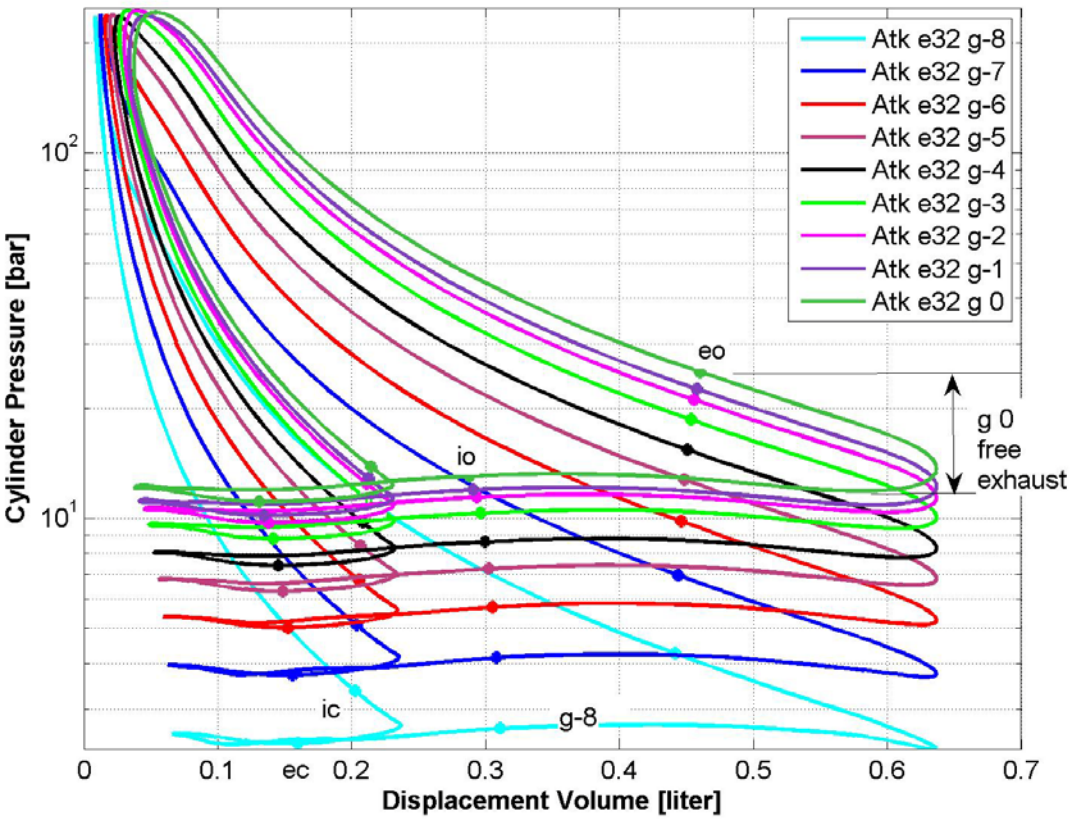

Fig. 22B: Pressure (logarithmic), Volume (log(p),V) - Diagram

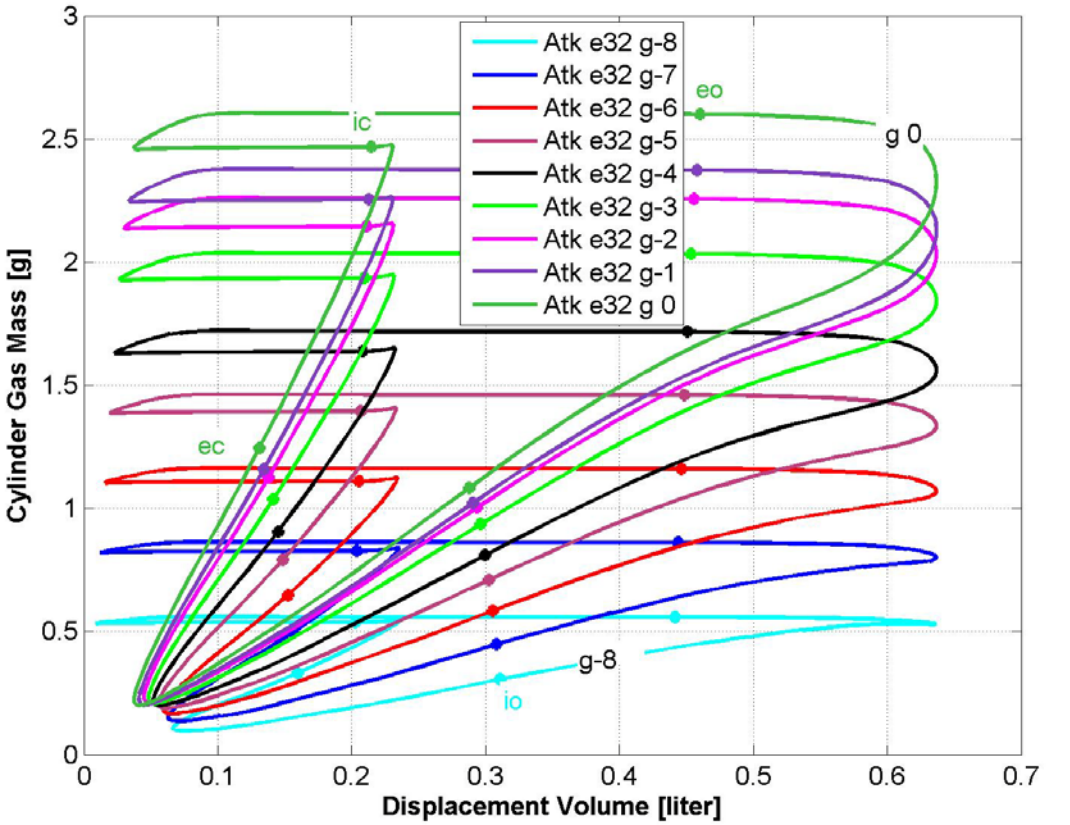

Fig. 23B: Fluid Mass, Volume (m,V) - Diagram

3.3. Evaluation of the highest IFCE values of the Seiliger and Atkinson cycles

3.3.1 The V,p,T ideal model for the open Seiliger and Atkinson cycles

Because in the case of the supercharged ICE, the number of parameters which influence the IFCE and BMEP is very high, the ask of achieving combinations of parameters which maximize the performances of the real (by BOOST) ICE cycle becomes very difficult. For these reasons, ideal models of the V,p,T-Seiliger and -Real-Atkinson cycles have been developed (see [4], [5], [6] and Appendix).
Modeling by means of V,p,T-cycles has the advantage of allowing users to generate ideal ICE cycles which model more closely the real cycles than the classic ideal V- and V,p-cycles by observing their mechanical (pressure) and thermal limits. A simple V-cycle (Otto cycle), where the heat is released only in an isochoric manner (i.e. by constant volume), generates unrealistically high levels of maximum pressure and temperature during the cycle. The attempt to limit the maximum pressure level leads to the classic V,p-cycle [7], [8], where the heat is released in an isochoric and isobaric (constant pressure) manner. The V,p-cycles (i.e. classic Seiliger cycles) leads, for example, to very high temperature levels in the case of fully loaded supercharged engines. These levels are completely unrealistic.

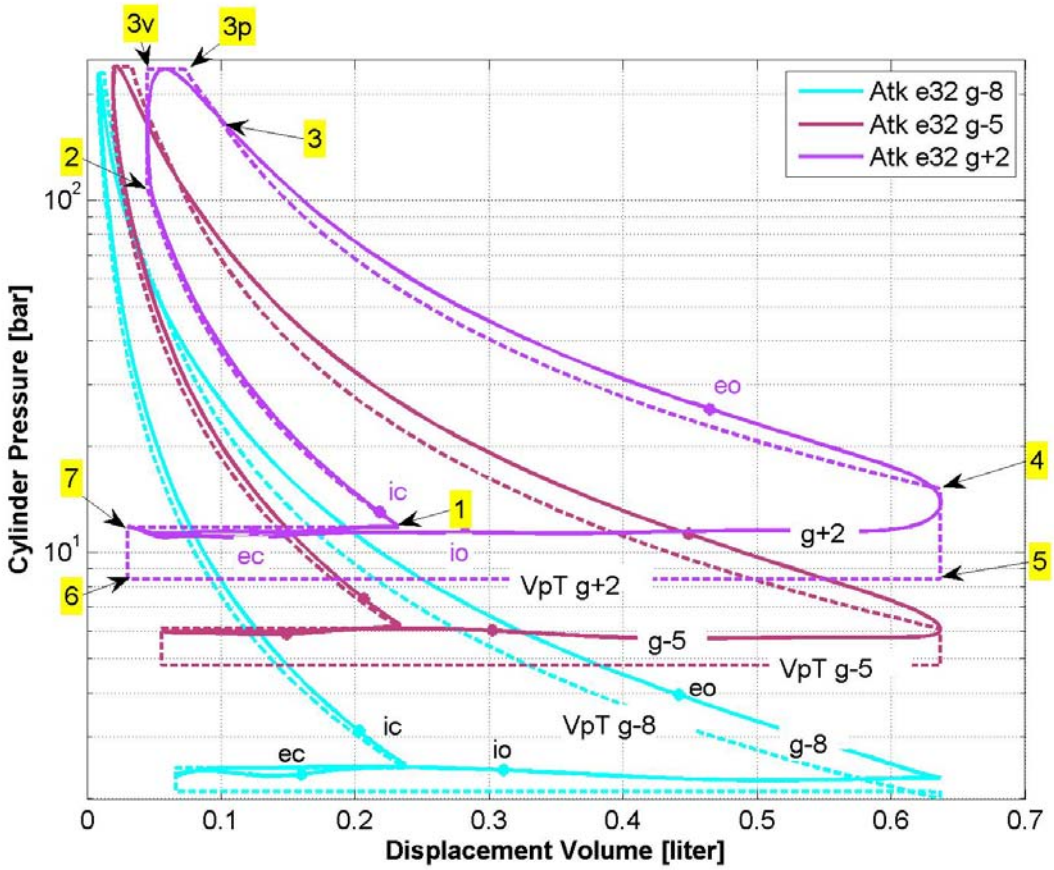

Fig. 24. Pressure (logarithmic), Volume (p,V) -Diagram for Boost (with Valves Timing) and V,p,T (dashed curves) for three Values of Parameter "g"

In the ideal V,p,T-cycle, the heat is partially released isochorically on the 2 – 3v change of states, isobarically on 3v – 3p and isothermally on 3p – 3 (see states noted in Fig. 24). The amounts of heat released isochorically and isobarically depend on the targets for maximum pressure and temperature of the cycle. The theoretical

background of this ideal open cycle (i.e. with gas exchange) is presented in detail in the Appendix.

In the ideal V,p,T model, the thermal properties of the working fluid (κ_c for the unburned and κ_e for the burned parts) are kept constant throughout the cycle. The entire fuel mass is added to the cylinder gas mass in the "3v" state of the cycle (see Fig. 24). The mass contribution of the exhaust rest gas part is also taken into consideration. The available heat (from fuel combustion) decreases by the amount of heat transferred to cylinder wall. In this case, the compression, combustion and expansion can be treated adiabatically. The backpressure behind the cylinder p_T (equivalent of the p_{MP12} from the BOOST model) is computed by means of energy balance at the turbocharger.
In order to be able to compare the simulation results, the following parameter are carried over from the BOOST to the V,p,T-model: p_C, T_C, p_{max}, T_{max}, m_1, m_f, κ_c, κ_e, Q_{wall} (see Appendix for their meaning).

The diagrams of cylinder pressure over displacement volume from Fig. 24 show a relatively good concordance for the high pressure part of the cycles. The heat release and heat transfer to cylinder wall are responsible for most of the differences. The V,p,T model features an optimal heat release, i.e. the maximum achievable isochorically and isobarically parts for reaching the target values for maximum pressure and temperature of the cycle. The gas exchange and turbocharging processes used in the V,p,T model are also optimal. The parameter and performances of the BOOST and V,p,T cycle simulations are shown in Fig. 25.

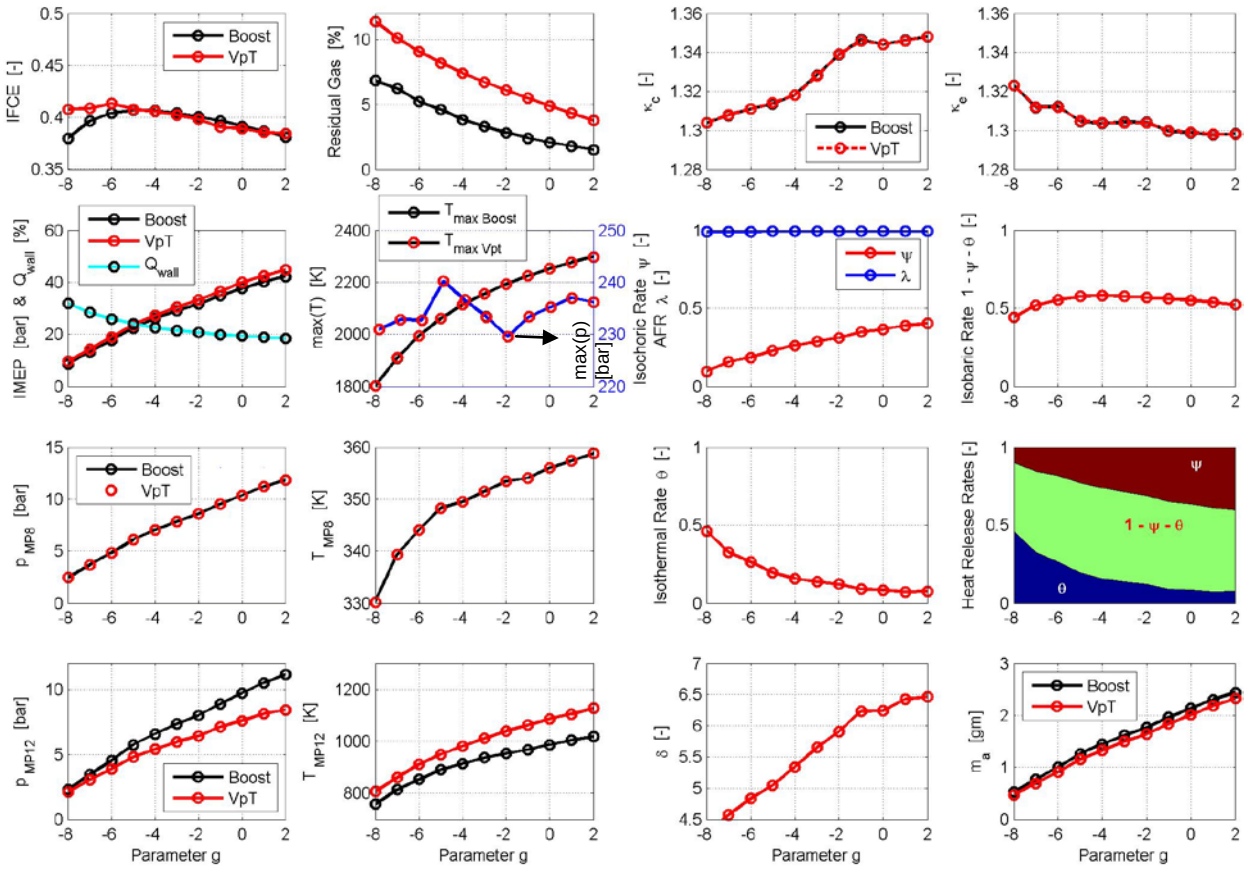

*Fig. 25 Parameter (left) and Performance (right) for **IC B** over Parameter "g"*

The IFCE values of the V,p,T model follow the upward movement of the VCR and VER values (the VCR and VER values of each "g" position of the crank shaft are presented in the legend of Fig. 13B) mainly because of the optimized heat release. The areas of ψ, 1-ψ-θ and θ from the diagram of the heat release rates, located on the right side of Fig. 25, explain this tendency.
The residual gas mass (i.e. rest exhaust gas rate per cycle) seen in the V,p,T simulation is the result of this ideal model. However, when initializing the V,p,T simulations, the model uses the values from BOOST simulations (i.e. as start values for a few iterations). The differences between the pressure and temperature behind the cylinder (i.e. in MP12 of the BOOST model, see Fig. 12) show the maximum potential of turbocharging in these operating points. The maximum cylinder pressure and temperature are kept identical in the BOOST and V,p,T simulations.

3.3.2 Comparison between the performances of the Seiliger and Real-Atkinson cycles by means of the V,p,T-model

The V,p,T model is used to simulate both cycles while preserving the same settings for:

- VCR ε_c,
- AFR λ,
- heat release rates (i.e. isochoric ψ, isobaric 1-ψ-θ and isothermal θ),
- heat transfer rate to the cylinder wall ξ_{wall},
- pressure at the end of compression p_2,
- boost pressure p_C and boost temperature T_C,
- free exhaust ratio $\phi_{ex} = p_4 / p_5$,
- overall turbocharger efficiency η_{TC}
- maximal cylinder displacement etc.

In this way, the big effort of optimizing all the BOOST model parameters (such as heat release, valves timing etc.) can be avoided and an accurate comparison between the performances of the Seiliger and Real-Atkinson cycles is enabled.

The asymmetrical crank mechanism used for these investigations enables the simultaneous variation of the volumetric ratios and (more reduced) of the piston strokes from Fig. 26. The maximum cylinder displacement remains nearly unchanged, when the VCR are varying between 5.1 and 18.1 (see Fig. 27).
The following figures present the simulation results for three values of the VCR for both the Seiliger and the Real-Atkinson cycles. The maximum pressure and temperature values of the cycles are not kept identical (see Fig. 28 to 30). In Fig 28, one can see that the free exhaust ratios ϕ_{ex} were kept identical. By keeping the exhaust ratios identical in all simulations, we can assure similar conditions for the cylinder exhaust and, thus, for the levels of the cylinder back pressure and temperature (i.e. equivalent to p_{MP12} and T_{MP12} from the BOOST model, see Fig. 12). The aspirated gas mass of the Seiliger cycle is nearly two times bigger as in the Atkinson cycles (see Fig. 31). As expected, the efficiency (i.e. IFCE) of the Seiliger cycle is lower than that of the Atkinson cycles because of the truncated expansion. The analysis of the T,s-diagrams from Fig. 32 give a rough graphical estimation, while Fig. 33 provides the required evidence.

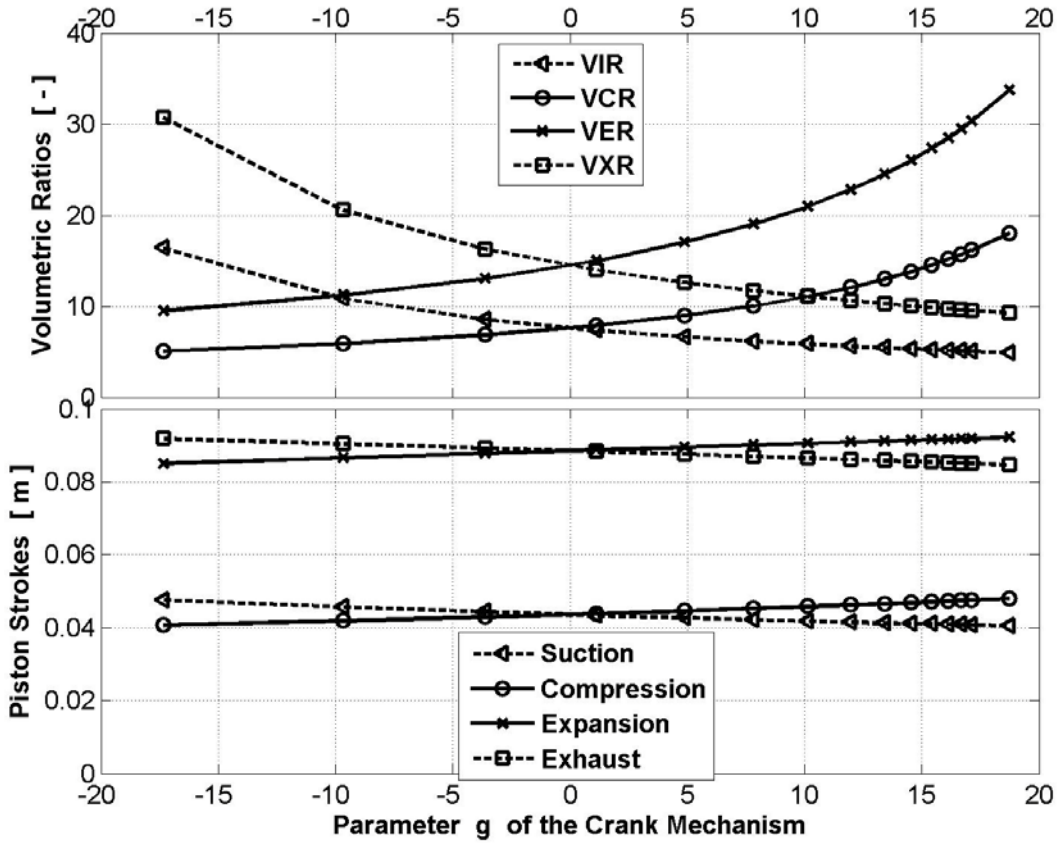

Fig. 26: Volumetric Ratios and Piston Strokes over Parameter "g"

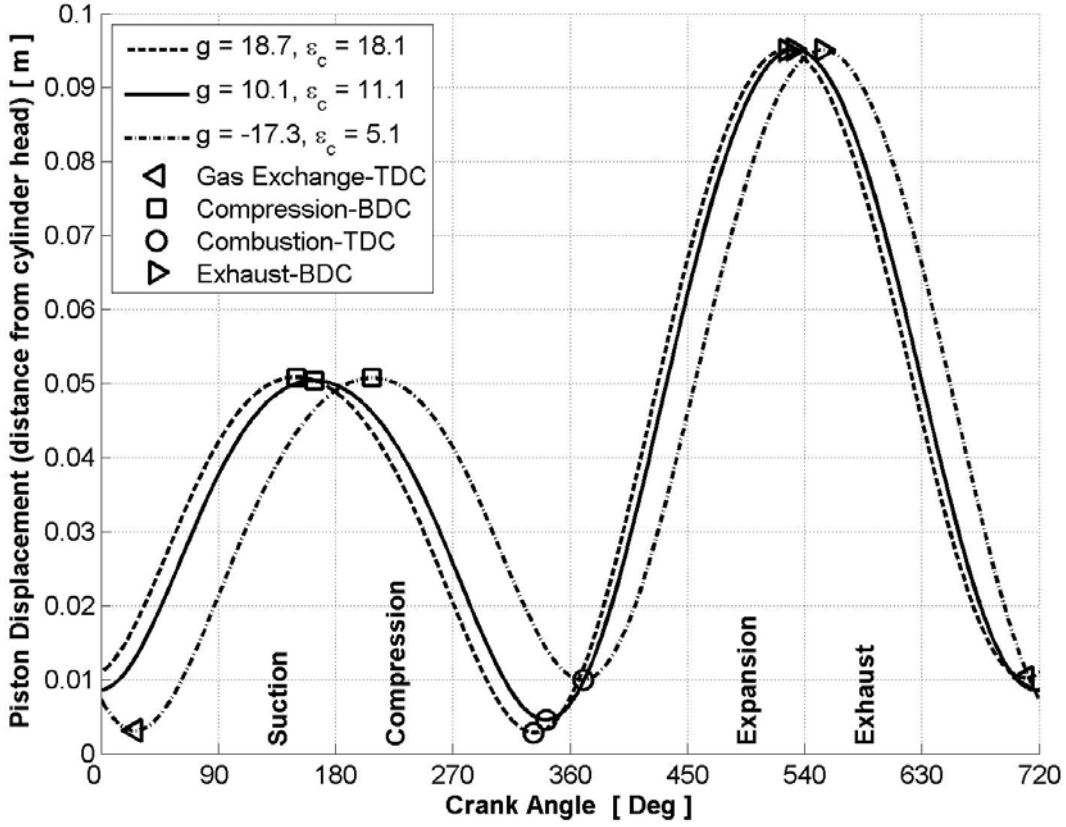

Fig. 27: Piston Displacement, Crank Angle -Diagram for three Values of "g"

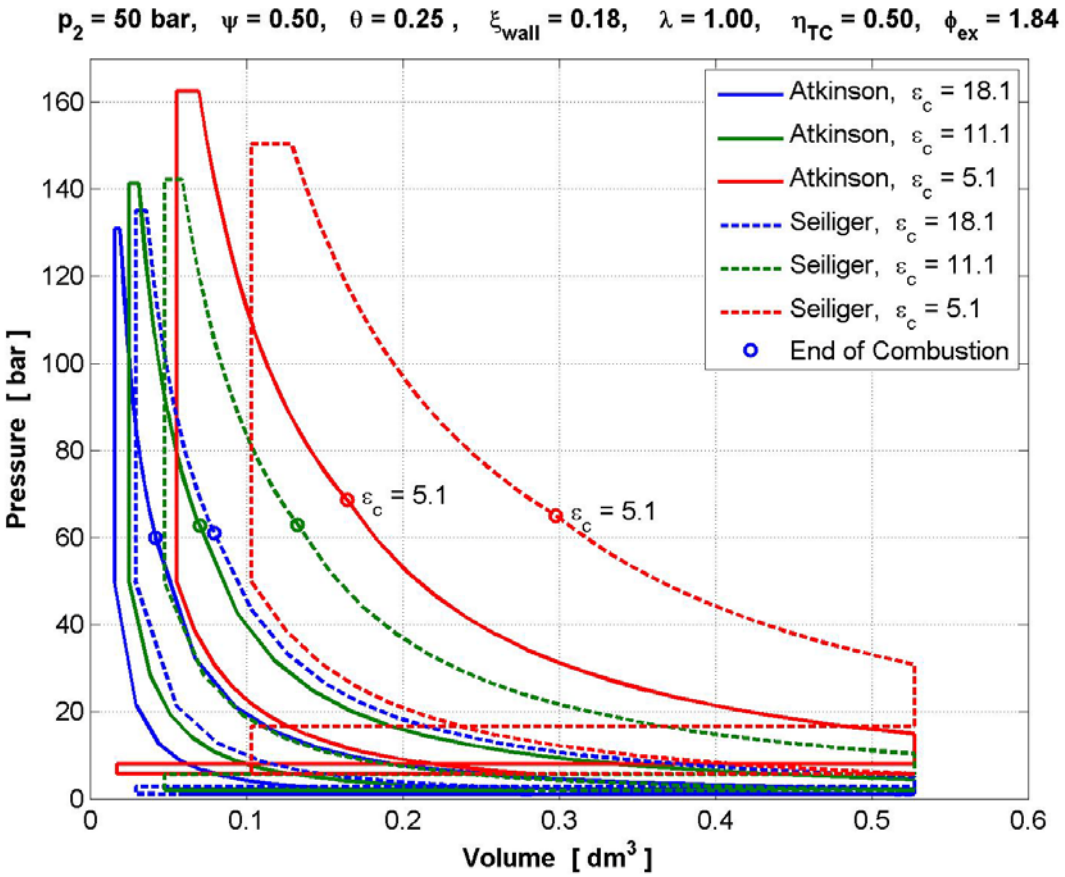

Fig. 28: Pressure, Volume (p,V) -Diagram regarding the VCR (ε_c) Variation

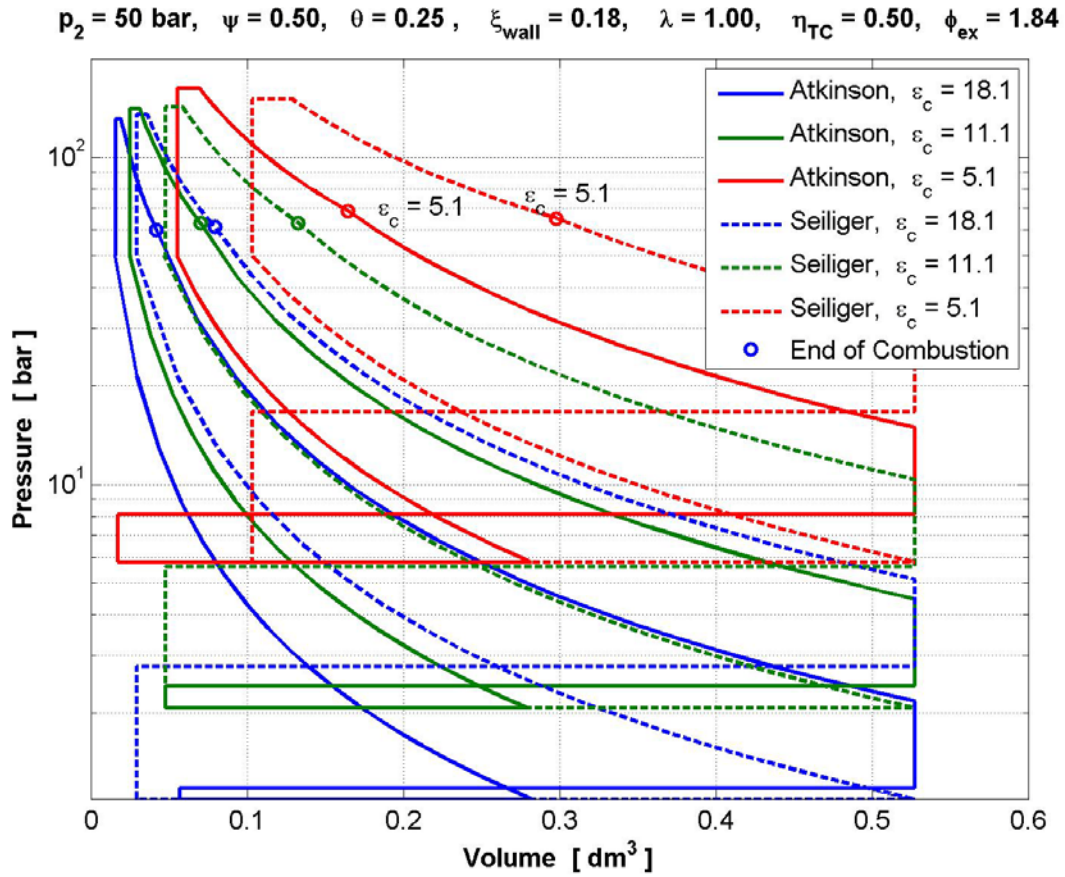

Fig. 29: Pressure (logarithmic), Volume - Diagram regarding the VCR (ε_c) Variation

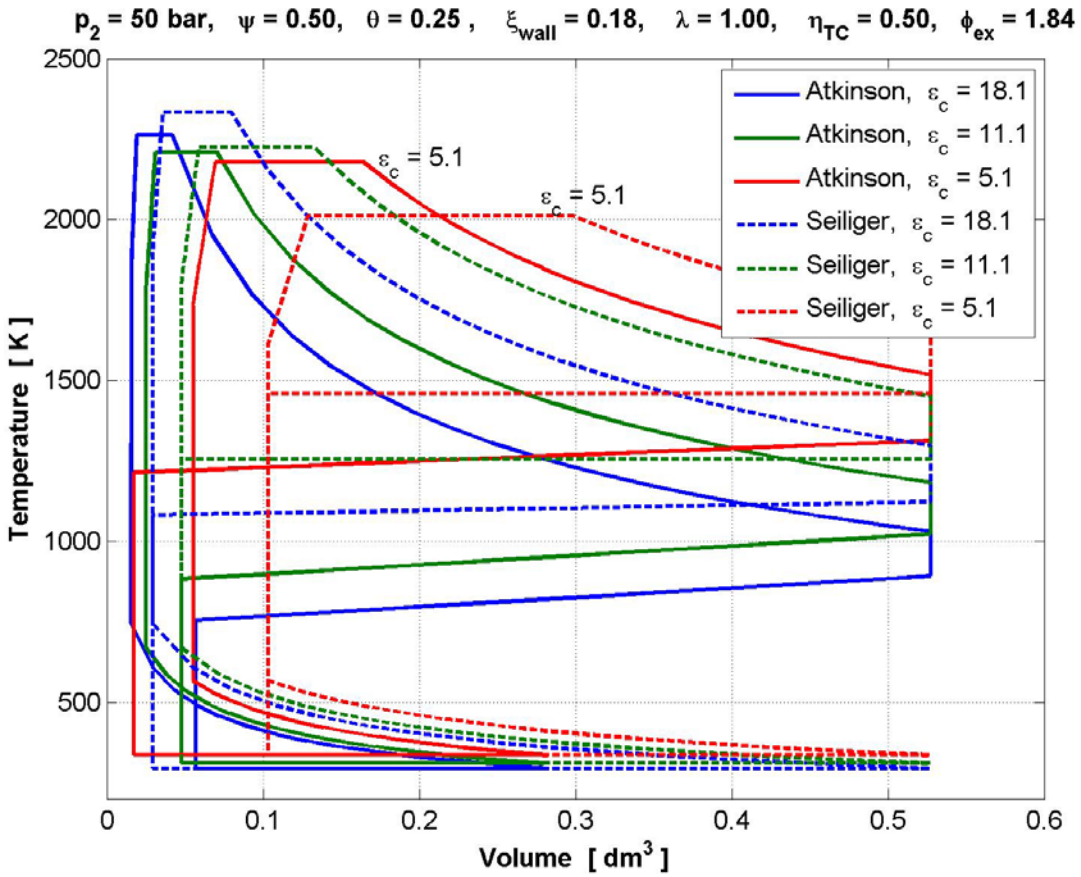

Fig. 30: Temperature, Volume (T,V) - Diagram regarding the VCR (ε_c) Variation

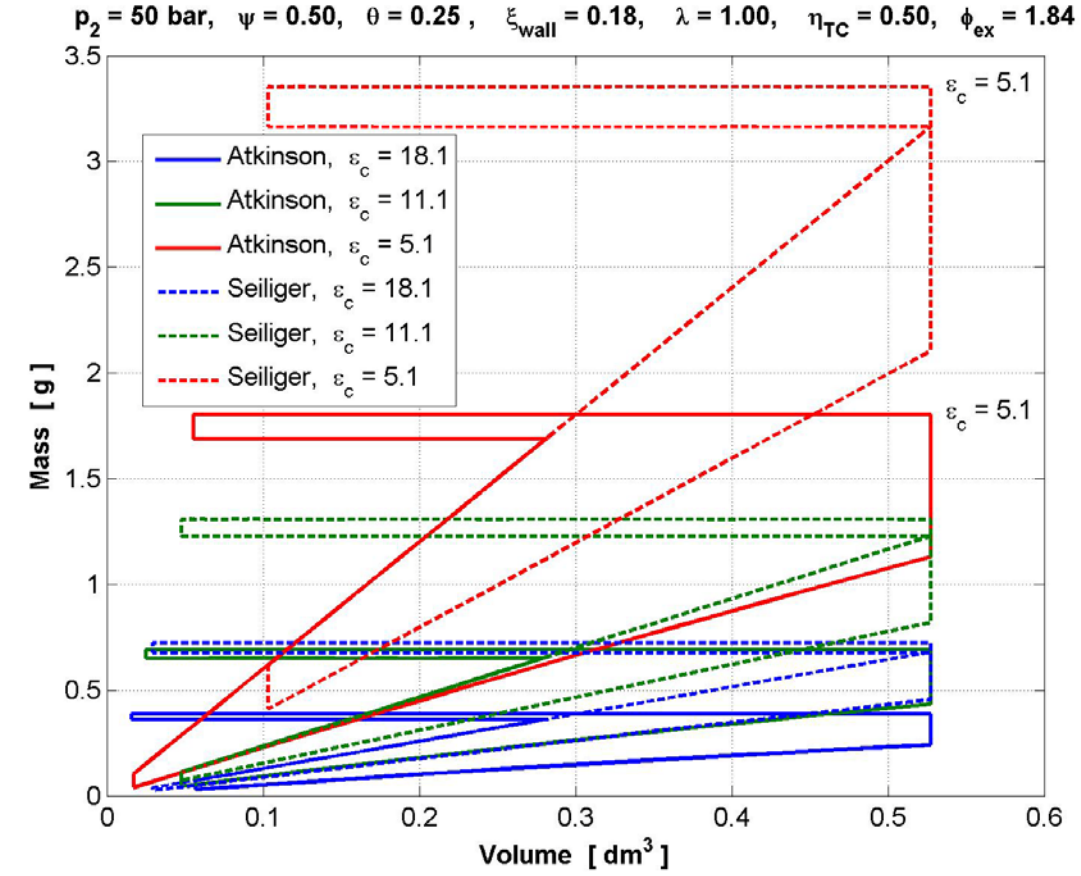

Fig. 31: Gas Mass, Volume (T,V) - Diagram regarding the VCR (ε_c) Variation

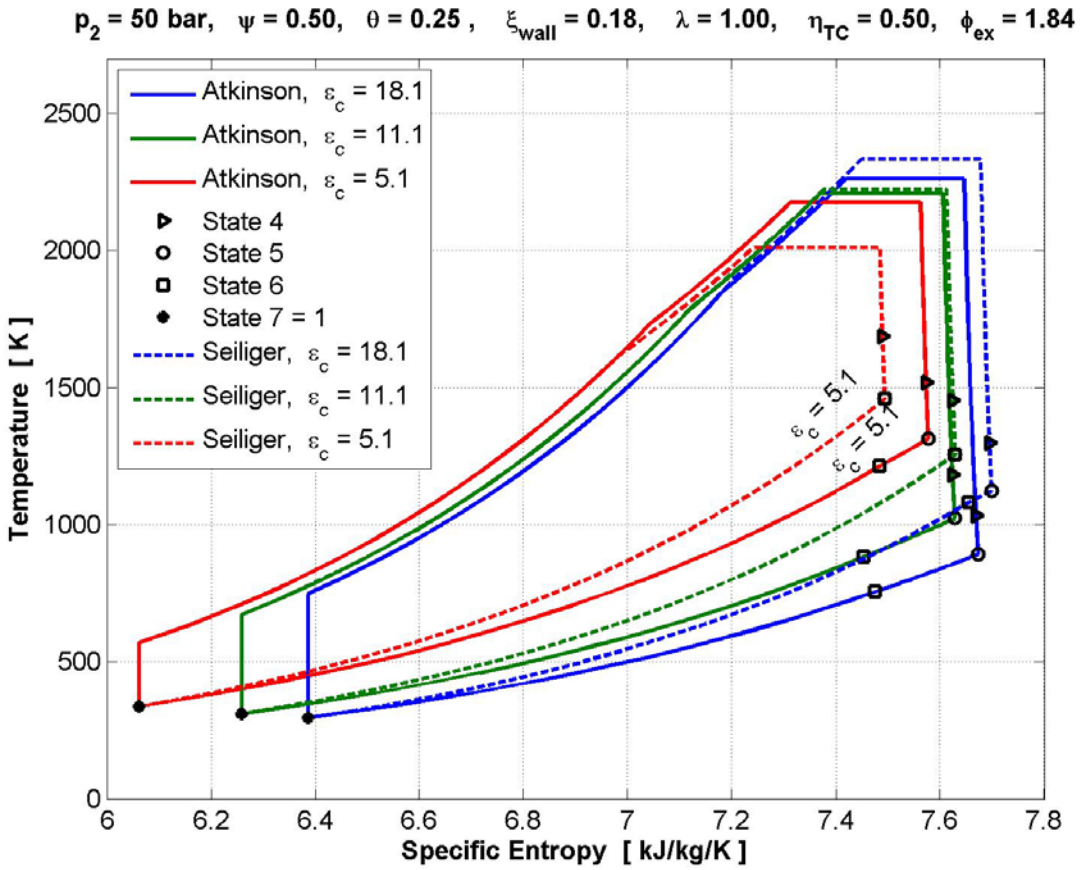

Fig. 32: Temperature, Specific Entropy (T,s) - Diagram regarding the VCR Variation

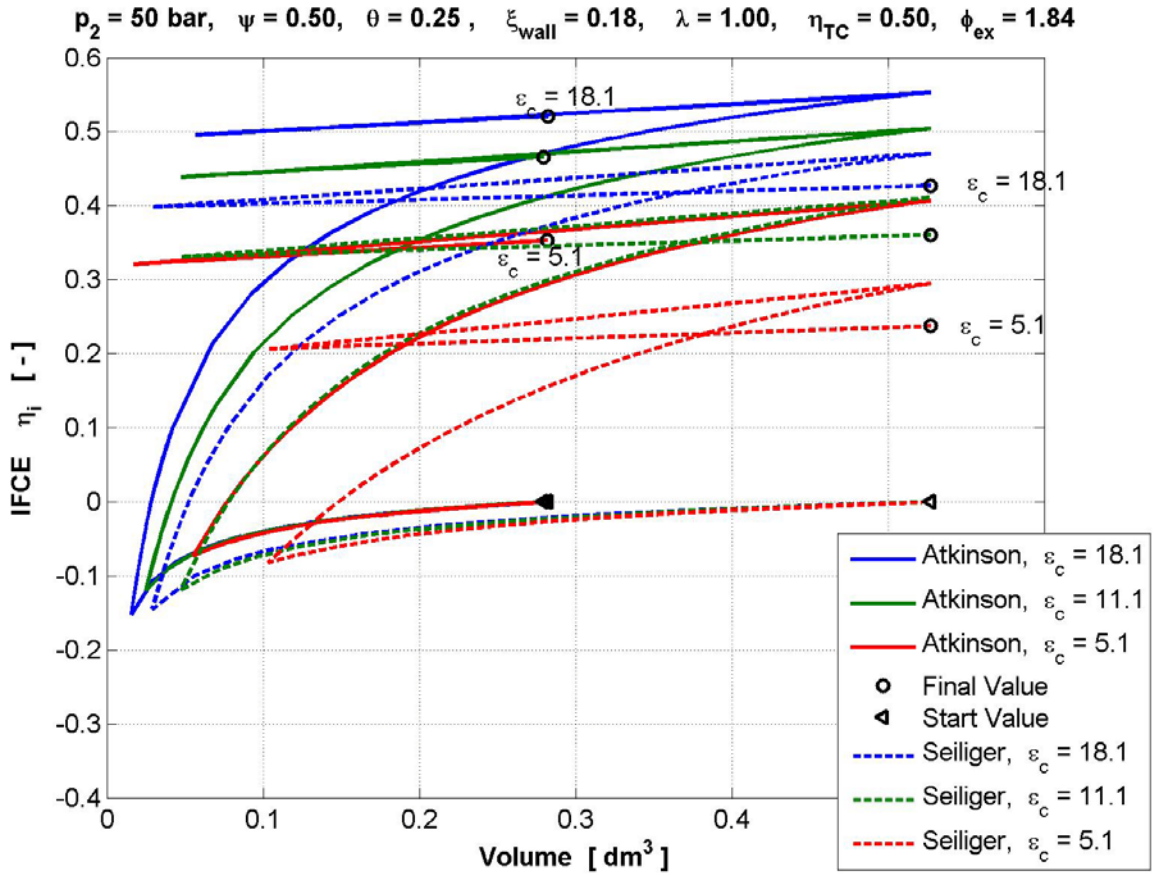

Fig. 33: IFCE, Volume (η_i,V) - Diagram regarding the VCR (ε_c) Variation

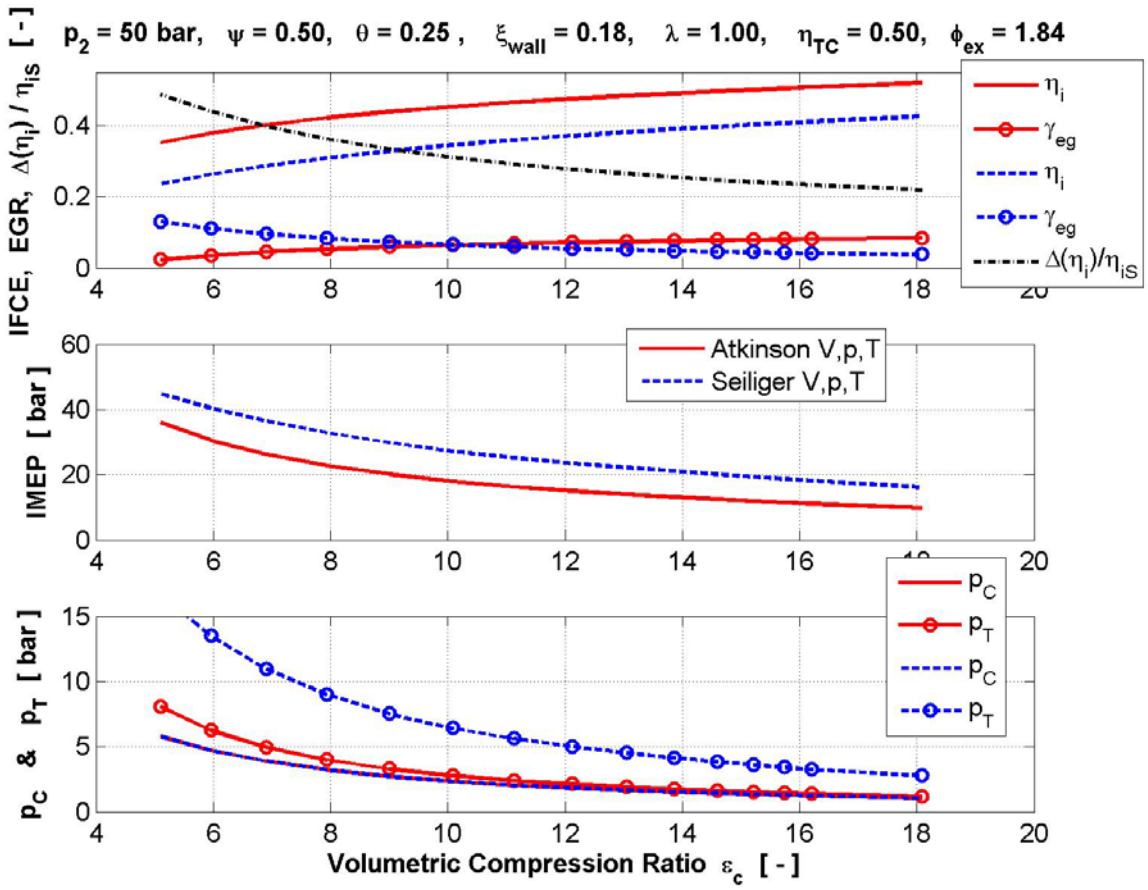

Fig. 34: Performances of the Atkinson and Seiliger Cycles regarding the VCR Variation

The performances of both cycles over the full variation range of VCR values are shown in Fig. 34. The boost pressure (p_C) and temperature are kept identical in both cycles (see below the diagram of Fig. 34). The cylinder back pressure (p_T) values are different because of the different gas mass to be exhausted in both cycles (see Fig. 31).
The IFCE improvement of the Real-Atkinson cycle when compared to the Seiliger cycle (i.e. $\Delta(\eta i)/\eta_{iS}$, see top diagram of Fig. 34) reaches more than 20% at all operating points and it increases by higher IMEP values.
The exhaust rest gas per cycle (EGR, see top diagram of Fig. 34) is decreased in the Atkinson cycle by increasing of the IMEP (see the middle diagram of Fig. 34). In this case, the available cylinder volume for the intake of fresh charge is bigger. On the other hand, the intake stroke increases with the reduction of the VCR (see Fig. 26 and Fig. 27). In conclusion both of these facts compensate partially by full load the shortened intake stroke of the Atkinson cycle. Accordingly, the IMEP reduction seen in the Atkinson cycle compared to the Seiliger cycle is not very significant (see the middle diagram of Fig. 34).

3.3. Strategies for Load Control

By using such an asymmetrical crank mechanism with a variable VCR, it is possible to achieve the Real-Atkinson cycles of turbocharged engines for part- and full loads even without the AFR variation (e.g. with stoichiometric) of AFR, the throttling or the excessive EGR (exhaust gas recirculation). If the asymmetrical crank mechanism

also enable the VCR variation for each cylinder separately, it is possible selectively to deactivate one or more cylinders by reducing the VCR and shut off of the fueling.

4. Conclusion

The implementation of the Real-Atkinson cycles for turbocharged engines using asymmetrical crank mechanisms offers the following advantages: a) relatively high IMEP, b) higher IFCE, leading to fewer CO_2 emissions and c) lower temperatures during the combustion stage, leading to fewer NO_x emissions.
In order to achieve this, the engine requires (in addition to variable valves timing etc.) the use of turbocharger systems with at least two stages, which must be adapted accordingly and controlled with the help of bypasses to maximize their performance. As a result, their optimization is very time consuming.
The comparisons between the V,p,T- and BOOST simulations shown in this paper indicate that this ideal V,p,T model can simulate a real model (in this case BOOST) relatively accurately and can predict correctly the upper limit of the cycle performances under the given engine operating conditions.

References

[1] Weinowski, R., Sehr A., Wedowski, S., Heuer, S., Hamm, T., Tiemann, C., Future downsizing of S.I. engines - potentials and limits of 2- and 3-cylinder concepts, Vienna Motor Symposium 2009

[2] Korte, V., Lumsden, G., Fraser, N., Hall, J., 30% higher efficiency at 50% less displacement, MTZ 2010

[3] Schutting, E, Neureiter, A, Fuchs, Ch., Schwarzenberger, T, Klell, M, Eichlseder, H, Kammerdiener, T, Miller- and Atkinson-Cycle for Supercharged Diesel Engines, MTZ 06 / 2007 (German)

[4] Gheorghiu, V.: CO2-Emission Reduction by Means of Enhancing the Thermal Conversion Efficiency of ICE Cycles, SAE International Powertrains, Fuels & Lubricants Congress, 2010, Rio de Janeiro, Brazil

[5] Gheorghiu, V.: Ultra-Downsizing of Internal Combustion Engines: Simultaneous Increasing of Thermal Conversion Efficiency and Power while Reducing Emissions, HEFAT Conference on Heat Transfer, Fluid Mechanics and Thermodynamics, 2011, Mauritius

[6] Gheorghiu, V.: Simultaneous Increasing of Thermal Conversion Efficiency and BMEP while Reducing Emissions, HEFAT Conference on Heat Transfer, Fluid Mechanics and Thermodynamics, 2012, Malta

[7] Heywood, JB, Internal Combustion Engine Fundamentals, MacGraw-Hill Book Company, 1988

[8] Pischinger, A., Kraβnig, G., Taucar, G., & Sams, Th., Thermodynamic of Internal Combustion Engines (German), Springer-Verlag, Wien New York, 1989

Appendix

Symbol	Meaning	Units
$\varepsilon_c = \frac{V_1}{V_2} = \frac{V_{in}}{V_c}$	volumetric compression ratio	-
$\varepsilon_e = \frac{V_5}{V_2} = \frac{V_e}{V_c}$	volumetric expansion ratio	-
$\varepsilon_i = \frac{V_1}{V_7} = \frac{V_{in}}{V_{out}}$	volumetric intake ratio	-
$\varepsilon_x = \frac{V_5}{V_6} = \frac{V_e}{V_{out}}$	volumetric exhaust ratio	-
$V_c = V_2 = V_{3v}$	cylinder volume at end of compression	m^3
$V_e = V_4 = V_5 = V_{max}$	cylinder volume at end of expansion	m^3
$V_{out} = V_6 = V_7$	cylinder volume at end of emptying	m^3
$V_{disp} = V_{max} \cdot \left(1 - \min\left(\frac{1}{\varepsilon_e}, \frac{1}{\varepsilon_x}\right)\right)$	cylinder displacement	m^3
$p_{max} = p_{3v} = p_{3p}$	maximal pressure on cycle	Pa
$T_{max} = T_{3p} = T_3$	maximal temperature on cycle	K
$p_1 = p_C$	cylinder pressure in state 1	Pa
$T_1 = T_C$	cylinder temperature in state 1	K
$m_1 = \frac{p_1 \cdot V_1}{m_1 \cdot T_1}$	cylinder gas mass in state 1	kg
$V_1 = V_{max} \cdot \frac{\varepsilon_c}{\varepsilon_e}$	cylinder volume in state 1	m^3
$m_a = m_1 \cdot \frac{\varepsilon_x - 1}{\varepsilon_x}$	aspirated charge mass per cycle	kg
$m_{max} = m_1 + m_f$	maximal gas mas on cycle	kg
$m_f = \frac{m_1 \cdot (1 - \gamma)}{\lambda \cdot L_{st}}$	fuel mass per cycle	kg
γ	exhaust rest gase rate per cycle	-
λ	air-exces ratio (AFR)	-
L_{st}	stoichiometric air requirement ratio	$\frac{kg}{kg}$
κ_c, κ_e	isentropic exponents and	-
$c^\circ_{p.c}, c^\circ_{v.c}$ $c^\circ_{p.e}, c^\circ_{v.e}$	isobaric (p) & isochoric (v) specific heat capacities on compression (c) resp. expansion (e)	$\frac{J}{kg \cdot K}$
R	ideal gas constant	$\frac{J}{kg \cdot K}$
H_u, H_{vap}	fuel lower heating & vaporisation heat values	$\frac{J}{kg}$
$Q_{rel} = m_f \cdot H_u$	cylinder released heat	J
η_b	released fuel energy completeness	-
Q_{wall}	heat transfer to cylinder wall	J

Abbreviations

AFR	Air-Fuel Ratio
BMEP	Break Mean Pressure
CA	Crank Angle
EOP	Engine Operating Point
ICE	Internal Combustion Engine
IFCE	Indicated Fuel Conversion Efficiency
IMEP	Indicated Mean Pressure
MPx	Measuring Point x in BOOST model
SOC	Start of Combustion
TC	Turbocharger
Tx	Turbine x (here x = 1..3)
VCR	Volumetric Compression Ratio
VER	Volumetric Expansion Ratio
VIR	Volumetric Intake Ratio
VXR	Volumetric Exhaust Ratio
V,p,T	Model of an ideal cycle where the heat is partially released isochorically, isobarically and isothermally
eo	Exhaust Valve Opening
ec	Exhaust Valve Closing
io	Intake Valve Opening
ic	Intake Valve Closing
μ_{Tx}	Discharge Coefficient of Turbine x

Symbol	Meaning	Units
$Q_{disp} = Q_{rel} \cdot \eta_b + Q_{wall}$	disposable heat on cycle	J
p_C	charge pressure after cooler	Pa
T_C	charge temperature after cooler	K
p_T	pressure before turbine	Pa
T_T	temperature before turbine	K
p_u	ambient pressure	Pa
$\delta = \frac{Q_{disp}}{m_{max} \cdot c°_{v.c} \cdot T_1}$	relative released heat as measure of engine load	-
$Q_{disp.v}$	isochoric part of Q_{disp}	J
$\psi = \frac{Q_{disp.v}}{Q_{disp}}$	isochoric released heat fraction	-
$Q_{disp.t}$	isothermal part of Q_{disp}	J
$\theta = \frac{Q_{disp.t}}{Q_{disp}}$	isothermal released heat fraction	-
$1 - \psi - \theta = \frac{Q_{disp.p}}{Q_{disp}}$	isobaric released heat fraction	-
$\phi_{ex} = \frac{p_4}{p_5}$	pressure ratio for free exhaust	-
$Q_{disp.p}$	isobaric part of Q_{disp}	J
$\eta_i = \frac{-W_{cycle}}{Q_{rel}}$	indicated fuel conversion efficiency IFCE	-
W_{cycle}	work on the all cycle	J
$p_i = \frac{-W_{cycle}}{V_{disp}}$	indicated mean pressure IMEP	Pa
$\eta_{sC}, \eta_{sT}, \eta_{TC}$	isentropic efficiency of compressor, turbine and turbocharger	-
W_{TTu}	turbine work between p_T and p_u	J
W_{CuC}	compressor work between p_u and p_C	J

Formula for the ideal V,p,T-model

$$m_2 = m_1 \qquad p_2 = p_1 \cdot \varepsilon_c^{\kappa_c} \qquad V_2 = \frac{V_1}{\varepsilon_c} \qquad T_2 = T_1 \cdot \varepsilon_c^{\kappa_c - 1}$$

$$m_{3v} = m_{max} = m_1 \cdot \left(1 + \frac{1-\gamma}{\lambda \cdot L_{st}} \cdot \frac{\varepsilon_x - 1}{\varepsilon_x}\right)$$

$$p_{3v} = p_{max} \qquad V_{3v} = V_2 \qquad T_{3v} = \frac{m_1}{m_{max}} \cdot \frac{p_{max}}{p_C} \cdot \frac{T_1}{\varepsilon_c}$$

$$\theta = 1 - \psi - \frac{\kappa_e \cdot (\kappa_c - 1)}{(\kappa_e - 1) \cdot \delta} \cdot \left(\frac{T_{max}}{T_1} - \frac{m_1}{m_{max}} \cdot \frac{p_{max}}{p_C} \cdot \frac{1}{\varepsilon_c}\right)$$

$$m_{3p} = m_{max} \qquad V_{3p} = V_{3v} \cdot \frac{T_{max}}{T_{3v}} \qquad T_{3p} = T_3 = T_{max}$$

Formula for the ideal V,p,T-model

$$V_4 = V_{max} \qquad p_4 = p_3 \cdot \left(\frac{V_3}{V_4}\right)^{\kappa_e} \qquad T_4 = T_3 \cdot \left(\frac{V_3}{V_4}\right)^{\kappa_e - 1}$$

$$p_5 = \frac{p_4}{\phi_{ex}} \qquad \text{where e.g.} \qquad \phi_{ex} = \left(\frac{2}{1+\kappa_e}\right)^{\frac{\kappa_e}{\kappa_e - 1}}$$

$$W_{CuC} = c°_{p.c} \cdot \frac{m_a \cdot T_u}{\eta_{sC}} \cdot \left[\left(\frac{p_C}{p_u}\right)^{\frac{\kappa_c - 1}{\kappa_c}} - 1\right]$$

$$W_{TTu} = \eta_{sT} \cdot (m_a + m_f) \cdot c°_{p.e} \cdot T_T \cdot \left[1 - \left(\frac{p_u}{p_T}\right)^{\frac{\kappa_e - 1}{\kappa_e}}\right]$$

$$W_{CuC} = W_{TTu} \qquad k_1 = \eta_{TC} \cdot \frac{1 - \gamma + \lambda \cdot L_{st}}{\lambda \cdot L_{st}} \cdot \frac{\kappa_e}{\kappa_e - 1} \cdot \frac{\kappa_c - 1}{\kappa_c} \cdot \frac{1}{T_u}$$

$$p_C = p_u \cdot \left[1 + k_1 \cdot T_4 \cdot \left[\left(\frac{p_5}{p_4}\right)^{\frac{\kappa_e - 1}{\kappa_e}} - \left(\frac{p_u}{p_4}\right)^{\frac{\kappa_e - 1}{\kappa_e}}\right]^{\frac{\kappa_c}{\kappa_c - 1}}\right]$$

$$T_5 = T_4 \cdot \left(\frac{p_5}{p_4}\right)^{\frac{\kappa_e - 1}{\kappa_e}} \qquad V_5 = V_{max} \qquad p_5 = p_T \qquad T_T = T_5 \qquad m_5 = \frac{p_5 \cdot V_5}{R \cdot T_5}$$

$$p_6 = p_5 \qquad V_6 = \frac{V_{max}}{\varepsilon_x} \qquad T_6 = (2 \cdot T_5 - T_4) \cdot k_{T6}$$

$$m_6 = \frac{p_6 \cdot V_6}{R \cdot T_6}$$

$$W_{cycle} = \frac{p_C \cdot V_{max}}{\kappa_c - 1} \cdot \frac{\varepsilon_c}{\varepsilon_e} \cdot \left(\varepsilon_c^{\kappa_c - 1} - 1\right) + \frac{p_{max} \cdot V_{max}}{\varepsilon_e} \ldots$$
$$+ (-m_{max}) \cdot R \cdot T_{max} - \theta \cdot \delta \cdot \frac{m_{max} \cdot R \cdot T_1}{\kappa_c - 1} \ldots$$
$$+ \frac{m_{max} \cdot R \cdot T_{max}}{\kappa_e - 1} \cdot \left[\left(\frac{V_3}{V_{max}}\right)^{\kappa_e - 1} - 1\right] \ldots$$
$$+ p_T \cdot V_{max} \cdot \frac{\varepsilon_x - 1}{\varepsilon_x} - p_C \cdot V_{max} \cdot \left(\frac{\varepsilon_c}{\varepsilon_e} - \frac{1}{\varepsilon_x}\right)$$

$$k_{T6} = \frac{\text{area}(T, s) \cdot m_{max}}{W_{cycle}} \qquad \gamma = \frac{m_6}{m_1} \qquad \text{iterative}$$